

The Paleoproterozoic Nattanen-type granites in northern Finland and vicinity – a postcollisional oxidized A-type suite



ESA HEILIMO^{1)*}, JAANA HALLA²⁾, LAURA S. LAURI¹⁾, O. TAPANI RÄMÖ¹⁾,

HANNU HUHMA³⁾, MATTI I. KURHILA¹⁾, AND KAI FRONT⁴⁾

1) Department of Geology, P.O. Box 64, FI-00014 University of Helsinki, Finland

2) Geological Museum, Finnish Museum of Natural History, P.O. Box 11, FI-00014 University of Helsinki, Finland

3) Geological Survey of Finland, P.O. Box 96, FI-02151 Espoo, Finland

4) VTT, P.O. Box 1000, Espoo, FI-02044 VTT, Finland

Abstract

The ~1.8 Ga Nattanen-type granites in the Finnish Lapland and western Kola Peninsula are found as several relatively small, high-level, discordant plutons that are easily discernible as weak maxima on aeromagnetic maps. We present U–Pb mineral isotope data on the Finnish plutons. The concordia ages are in the 1.79–1.77 Ga range and there is little evidence for inheritance. Initial radiogenic isotope compositions (our common-Pb data combined with previously published whole-rock Nd and Hf data) imply a major, yet varying, Archean source component. Elemental geochemical data on five Finnish intrusions (the Nattanen stock, the Tepasto and Pomovaara complexes, the Riestovaara and Vainospää batholiths), as well as, associated dyke rocks allow the Nattanen-type granites to be classified as oxidized A-type granites. Their petrogenesis may be related to partial melting of the lower crust by mafic underplating (extensional setting) or as a result of thermal relaxation in thickened crustal setting.

Key words: granites, A-type granites, geochemistry, genesis, absolute age, isotopes, U/Pb, Pb/Pb, Paleoproterozoic, Lapland Province, Finland.

* Corresponding author email: esa.heilimo@helsinki.fi

I. Introduction

Since their recognition in the 1920's (Mikkola, 1928), the Nattanen-type granites in northern Finland and adjacent Russia have remained a rare example of highly discordant, post-orogenic, high-level granite plutons in the far north of the Fennoscandian shield. These plutons (the Nattanen stock, the Tepasto and Pomovaara complexes, the Riestovaara and Vainospää batholiths on the Finnish side; the Juvoaivi stock and

the Litsa-Aragub complexes on the Russian side) are younger (~1.77–1.80 Ga; Kouvo et al., 1983; Meriläinen, 1976, Vetrin et al., 2006; this study) than their immediate country rocks and are found as multiple intrusions within the Neoarchean and early Paleoproterozoic metamorphic bedrock of Finnish Lapland and vicinity. The Nattanen-type granites are characterized by miarolitic cavities, evolved com-

positions, and an oxidized redox budget (titanite and magnetite as conspicuous minor phases) (Haapala et al., 1987; Front et al., 1989; Lehtiö, 1993). They are also associated with evolved rhyolitic dyke rocks and minor Mo-mineralization. Geochemically, the Nattanen-type granites have previously been considered mainly I-type, but some of the more evolved intrusive phases of the plutons may show A- or S-type characteristics (Front et al., 1989). Available isotope data (Lu–Hf, Sm–Nd, Pb–Pb) imply a major Archean source component for these granites (Patchett et al., 1981; Kouvo et al., 1983; Huhma, 1986). In this paper we present whole-rock and K-feldspar Pb–Pb as well as zircon, monazite, and titanite U–Pb isotope data on the Nattanen-type intrusions. We use these data to examine the temporal evolution of the granites and refine their source model. We also elaborate on existing whole-rock elemental geochemical data in order to enhance their typological significance.

2. Geologic setting

The northern part of the Fennoscandian shield is composed of several Archean crustal domains (Karelia, Kola, and Norrbotten, inset in Fig. 1; e.g., Lahtinen et al., 2005) and intracratonic basins of Paleoproterozoic supracrustal rocks that were intruded by several generations of mafic and felsic intrusive rocks (e.g., Hanski & Huhma, 2005; Nironen, 2005). Extensional tectonics prevailed in the early Paleoproterozoic, fracturing the Archean Karelia craton from ca. 2.45 Ga onwards and creating gradually deepening basins that were subsequently filled with supracrustal material (e.g., Lehtonen et al., 1998; Hanski & Huhma, 2005). The long extensional period ended by ca. 1.93 Ga when the Karelia and Kola domains collided (the Lapland-Kola orogeny) and the Lapland granulite belt (LGB) was formed (Daly et al., 2001; Lahtinen et al., 2005 and references therein; Fig. 1). The Lapland-Kola orogeny was followed by the collision of Karelia with the Norrbotten domain (Fig. 1 inset) from the present northwest at ca. 1.92 Ga (Lahtinen et al., op.cit.). The Karelia-Norrbotten collision thrusted the volcanic rocks of the Kittilä group on to

the Karelian domain (Lehtonen et al., 1998; Hanski & Huhma, 2005; Lahtinen et al., 2005; Patison et al., 2006). The final major accretional event was the formation of the Svecofennian domain in the south (e.g., Lahtinen et al., op. cit.).

Several granitoid-forming events (most of them collisional) have been recognized in the northern part of the Fennoscandian shield (e.g., Nironen, 2005 and references therein). However, the oldest known Paleoproterozoic granites of ca. 2.1 Ga age cannot be connected to any presently known collision (Huhma, 1986; Rastas et al., 2001; Ahtonen et al., 2007). Granitoids with ages in the 1.95–1.91 Ga range (and classified as preorogenic by Nironen, 2005) are known within the Hetta complex (Fig. 1; Rastas et al., 2001) as well as intruding the Kittilä group (Huhma, 1986; Rastas et al., 2001; Ahtonen et al., 2007), the Lapland granulite belt (LGB; Tuisku & Huhma, 2006), and in the Inari complex (Meriläinen, 1976). Synorogenic, ca. 1.89–1.86 Ga granitoids intruded the older rock types mostly in Sweden and western Lapland, and they are coeval with the Svecofennian granitoids farther south (e.g., Lehtonen et al., 1998; Bergman et al., 2001; Nironen, 2005). The last granite-forming phase occurred between 1.80 Ga and 1.76 Ga, producing the deformed migmatites, leucogranites, and appinitic intrusions (Mutanen & Väänänen, 2004) of the central Lapland granitoid complex (CLGC; the late-orogenic granites of Nironen, 2005; see also Ahtonen et al., 2007), as well as the discordant Nattanen-type granite plutons.

3. The Nattanen-type granites

The Nattanen-type plutons are found in western, central, and northern Finnish Lapland. The location of these granite plutons seems to be largely controlled by crustal-scale fracture zones and they are found in all three blocks of the Archean crust (Figs. 1 and 2). The following description of the Nattanen, Tepasto, Pomovaara, and Riestovaara intrusions is mainly based on Front et al. (1989) and concerning ore minerals it is based on Lehtiö (1993); the Vainospää granite is described after Meriläinen (1976) and the



Fig. 1. Geological sketch map of northern Finland showing the location of the ~1.8 Ga Nattanen-type granites in Finnish Lapland and far northwest Russia. Modified from Korsman et al. (1997), and Haapala et al. (1987). Key to the intrusions: 1 = Tepasto; 2 = Pomovaara; 3 = Riestovaara; 4 = Nattanen; 5 = Vainospää; 6 = Juvoaivi; 7 = Litsa-Aragub. Key to the crustal units: IC = Inari complex; LGB = Lapland granulite belt; KA = Kittilä allochthon; HC = Hetta complex; CLGC = Central Lapland granitoid complex. Inset shows the location of the area relative to the Fennoscandian shield. KoD = Kola domain; KarD = Karelian domain; ND = Norbotten domain; SD = Svecofennian domain; TIB = Transscandinavian igneous belt; SSD = Southwest Scandinavian domain.

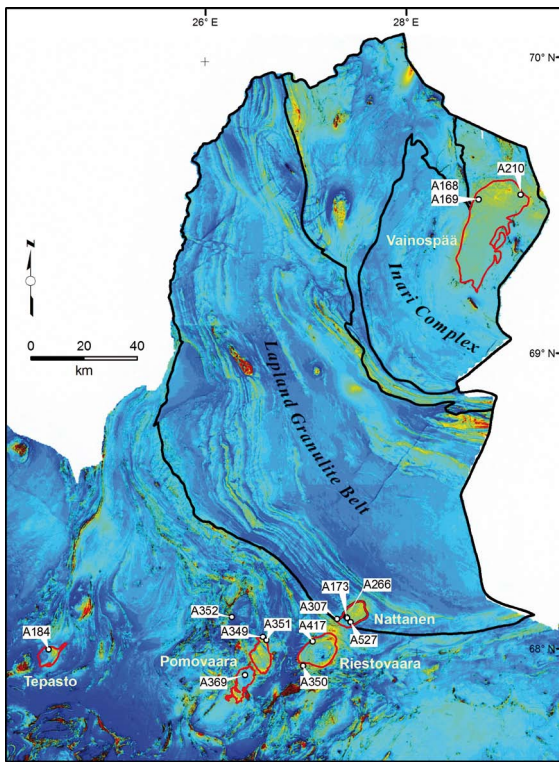


Fig. 2. Aeromagnetic map of northernmost Finland based on aeromagnetic data from the Geological Survey of Finland (GTK). The Nattanen-type granites are marked by moderate magnetic maxima. A-coded numbers denote isotope sample locations of this study.

Nattanen-type granites in Russia after Vetrin et al. (2006).

The Nattanen-type granites are typically unfoliated, medium- to coarse-grained monzogranites with allanite, zircon, and titanite as typical accessory minerals (Mikkola, 1941). The granite types of the plutons differ more in texture than in mineral composition. The main mineralogical and petrographic features of the Nattanen-type granites are summarized in Table 1.

3.1. Nattanen stock

The type intrusion of the Nattanen-type granites, the Nattanen stock (Fig. 3a), is mainly hosted by the LGB that is composed of alternating layers of psam-

mitic to pelitic migmatites and younger, ca. 1.92–1.91 Ga rocks of norite-enderbite series (Tuisku & Huhma, 2006; Tuisku et al., 2006). Most of the Nattanen stock consists of coarse-grained biotite granite. Medium-grained granite is found only in the southern parts where the pluton intrudes garnet-hornblende gneisses instead of granulites. The stock is surrounded and rarely cross-cut by numerous rhyolite dykes with several textural variants from banded to spherulitic.

3.2. Tepasto complex

The westernmost Nattanen-type intrusion, the Tepasto complex, is hosted by Paleoproterozoic granites and migmatites of the Hetta complex that are in turn surrounded by the volcanic rocks of the Kittilä group (e.g., Lehtonen et al., 1985, 1998; Korsman et al., 1997; Pakkanen, 1993; Rastas et al., 2001). The Tepasto complex consists of several different granite types that form a concentric stock (Fig. 3b). The biotite-bearing coarse-porphyritic granite of the outer part is intruded by biotite granite in the central part of the pluton. The youngest phase is aplite granite that cross-cuts and brecciates the other granite types. Zircon U–Pb age of 1802 ± 10 Ma (MSWD=7) was reported for the coarse-porphyritic granite of the Tepasto stock by Rastas et al. (2001). Several small Mo- and Cu-occurrences have been found associated with the Tepasto complex. Most of them are in contact with the aplite granite or in small greisens near them. Ore minerals include molybdenite, bornite, covellite, chalcopyrite, hematite, pyrrhotite, magnetite, pyrite, sphalerite, ilmenite, and goethite.

3.3. Pomovaara complex

The Pomovaara complex in central Lapland comprises three individual stocks: Lehtovaara, Pomovaara, and Tenniövaara (Fig. 3c; Front et al., 1989; Wennerström & Airo, 1998). The Lehtovaara stock is mainly composed of coarse-porphyritic granite and minor granite porphyry. The Pomovaara stock is a concentric multiphase pluton with biotite-bearing porphy-

Table 1. Summary of the major granite phases of the Nattanen-type granites in northern Finland, their mineralogy and main petrographic features.

Intrusion	Intrusion phase	Petrography	Mineralogy ¹⁾	References:
Nattanen stock	Coarse-grained granite	Unfoliated, homogeneous and coarse-grained monzogranite with rapakivi texture sensu lato.	Qtz, Kfs, Plg, Bt, Op, All, Apa, Zrc, Ms, Ser, Chl, Epi, Fl, Mon, Ilm, Tit, Go	Luukkonen, 1989; Front et al., 1989; Lehtiö, 1993
	Medium-grained granite	Unfoliated, homogeneous with miarolitic cavities ($\varnothing = 1\text{--}2$ mm).	Kfs, Plg, Qtz, Bt, Op, Zrc, Apa, All, Epi, Ms, Chl	
Tepasto complex	Coarse-porphyritic granite	Slightly foliated monzogranite with euhedral K-feldspar, plagioclase and quartz phenocrysts. Rapakivi texture in places.	Kfs, Plg, Qtz, Bt, ±Hbl, Op, Tit, Apa, Zrc, Fl, All, Chl, Epi, Ms, Ser	Front et al., 1989
	Biotite granite	Even-grained, medium-grained monzogranite. Biotite and plagioclase are oriented along a weak foliation. K-feldspar and plagioclase show micrographic and myrmekitic intergrowth textures.	Qtz, Kfs, Plg, Bt, Epi, Chl, Ser, Op, Tit, Apa, Zrc, Fl	
	Aplite granite	Medium-grained and even-grained, homogeneous, unfoliated monzogranite with a small amount of micas. Plagioclase typically shows myrmekitic texture.	Qtz, Kfs, Plg, Bt, Ms, Op, Tit, Apa, Hem, Epi, Ms, Chl	
Pomovaara complex	Porphyritic granite	K-feldspar and plagioclase megacrysts are euhedral. K-feldspars show occasional rapakivi-texture. Matrix is medium-grained and composed of feldspars, quartz and biotite.	Qtz, Kfs, Plg, Bt, Op, Tit, Epi, All, Apa, Zrc, Chl, Ms, Ser	Front et al., 1989
	Two-mica and biotite granites	Monzogranites with K-feldspar and plagioclase phenocrysts. Matrix is unfoliated and medium-grained in both granite types.	Qtz, Kfs, Plg, Bt ± Ms, Op, Tit, Epi, All, Apa, Zrc, Chl, Ser	
Riestovaara batholith	Coarse-porphyritic granite	K-feldspar and plagioclase megacrysts. K-feldspar is perthitic and plagioclase shows myrmekitic texture. Occasional rapakivi texture.	Qtz, Kfs, Plg, Bt ± Hbl, Mgt, Tit, All, Zrc, Apa, Epi, Chl, Ms	Front et al., 1989
	Porphyritic granite	The amount of feldspar megacrysts varies (5–20 %). K-feldspar megacrysts are perthitic.	Qtz, Kfs, Plg, Bt, Mgt, Tit, All, Apa, Zrc, Mon, Fl	
	Medium-grained granite	Even-grained granite with micrographic intergrowths.	Qtz, Kfs, Plg, Bt, Fl, Op, Tit, Apa, Zrc, All, Chl, Ms	
Vainospää batholith		Slightly foliated intrusion with two granite types: medium-grained, porphyritic type, and coarse-grained, slightly porphyritic type. Plagioclase is zoned and shows myrmekitic texture.	Kfs, Plg, Qtz, Bt, Chl, Apa, Zrc, Op, Tit, Fl, All, Preh, Car	Meriläinen, 1976; This study

¹⁾ Accessory minerals are in italics. Mineral abbreviations: All – Allanite, Apa – Apatite, Bt – Biotite, Car – Carbonate, Chl – Chlorite, Epi – Epidote, Fl – Fluorite, Go – Goethite, Hem – Hematite, Hbl – Hornblende, Ilm – Ilmenite, Kfs – K-feldspar, Mgt – Magnetite, Mon – Monazite, Ms – Muscovite, Op – Opaque minerals, Plg – Plagioclase, Preh – Prehnite, Qtz – Quartz, Ser – Sericite, Tit – Titanite, Zrc – Zircon.

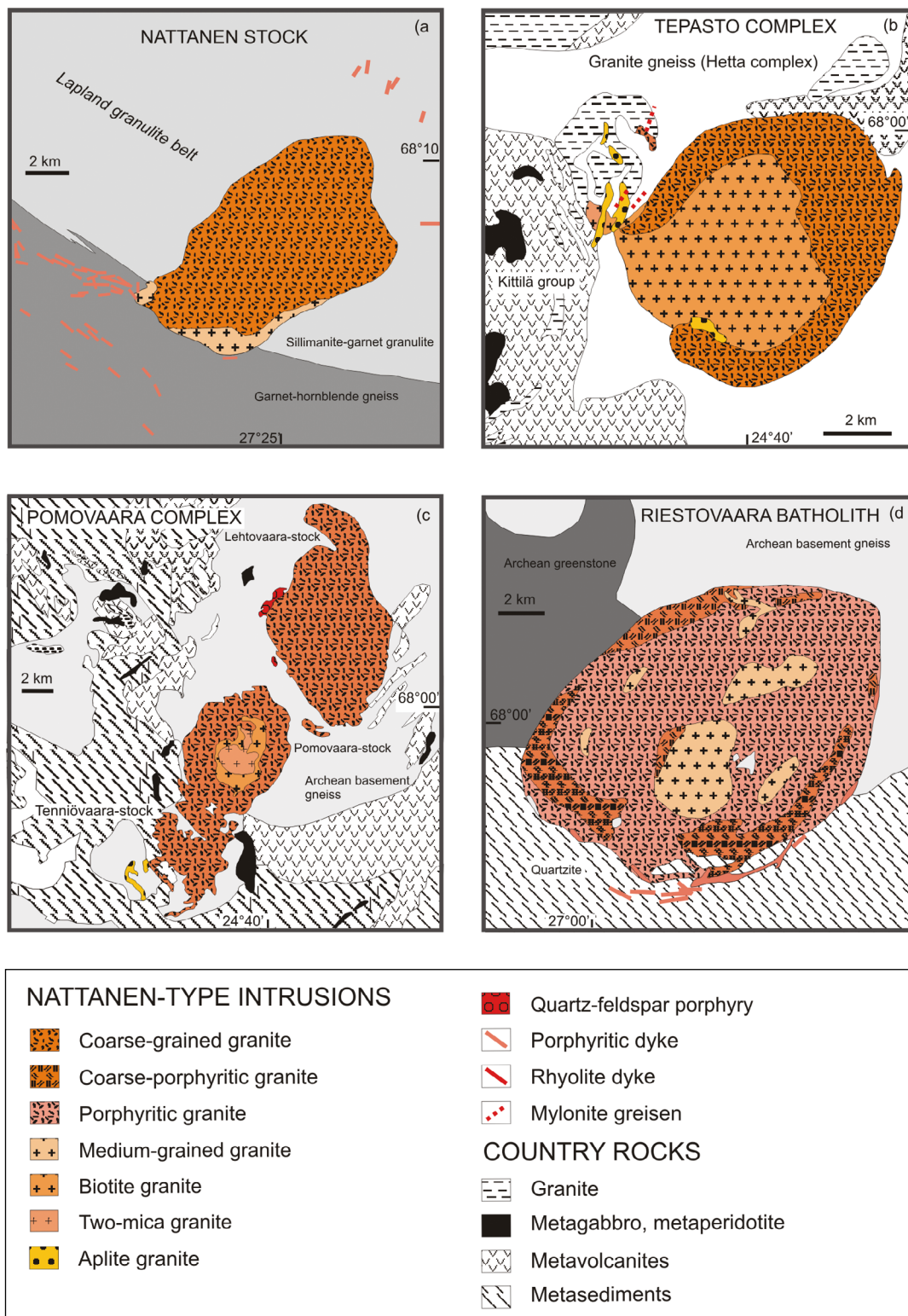


Fig. 3. Lithologic maps of the a) Nattanen stock; b) Tepasto complex; c) Pomovaara complex; d) Riestovaara batholith. The Nattanen-type intrusions modified from Front et al. (1989), country rocks adapted from Lehtonen et al. (1998) and Korsman et al. (1997).

ritic granite at the outer rim and biotite granite and two-mica granite in the central part. The Tenniövaara stock is composed of gray, porphyritic granite, which shows a weak orientation. Some porphyritic granite and aplite dykes are found outside the southern contact of the Tenniövaara stock. The Pomovaara complex is hosted by quartz-feldspar gneisses that have been considered to be Archean in age. However, the gneisses chiefly show heterogeneous Paleoproterozoic zircon populations, some of them with a rather well constrained magmatic age of ca. 2.49 Ga (Manninen et al., 2001). Minor Mo-mineralization is found in the Pomovaara complex and is associated with aplite and pegmatite dykes, quartz veins and mylonites. Ore minerals in the Mo-occurrences are molybdenite, chalcopyrite, pyrite, arsenopyrite, hematite, and goethite.

3.4. Riestovaara batholith

The Riestovaara batholith (Fig. 3d) is the largest Nattanen-type granite pluton on the southern side of the LGB. It is hosted by Archean granitic gneisses in the north and Paleoproterozoic quartzites, mica schists, gneisses, and metavolcanic rocks (2454 ± 5 Ma) in the south (Front et al., 1989; Manninen et al., 2001; Nironen & Mänttäri, 2003). The batholith consists of three granite types. Coarse-porphyritic granite is the oldest phase and forms an incomplete rim around the pluton. Most of the Riestovaara batholith consists of porphyritic granite, which is cross-cut in the central part of the intrusion by medium-grained granite. All granite types are biotite-bearing and undeformed, but magmatic foliation is observed in some outcrops. The southern part of the Riestovaara batholith hosts some granite porphyry dykes that are also present within the host rocks. Quartz-feldspar porphyry dykes, aplite dykes, and granodioritic to quartz dioritic dykes are also found.

3.5. Vainospää batholith

The Vainospää batholith is the largest of the Nattanen-type plutons in Finland. The thickness of the

batholith has been approximated to 6 km by three-dimensional gravity modeling (Elo et al., 1989). The batholith is hosted by the rocks of the Archean Inari terrane, on the NE side of the LGB (Fig. 1). Meriläinen (1976) coined the intrusion the Kynneljärvi-Vainospää granite and divided it into two sub-areas: the southern, gray Kynneljärvi granite and the northern Vainospää granite. The latter consists of slightly foliated, pink-gray, porphyritic granite and grey, coarse-grained granite.

3.6. Nattanen-type granites in Russia

Several Nattanen-type granite plutons are also found in the Russian territory east of the Vainospää batholith and the Nattanen stock (Fig. 1; e.g., Vetrin et al., 1975; Vetrin et al., 2006). The small Juvoaivi stock that intrudes the rocks of the LGB on the Russian side of the border was described and included in the Nattanen-type group by Mikkola (1928). The larger Litsa-Aragub complex farther north consists of at least six intrusions covering an area of 900 km^2 along a large fault zone that probably controlled their emplacement. The Juvoaivi and Litsa-Aragub granites show ages in the 1.79–1.76 Ga range (Vetrin et al., 2006). The magmatic association in the Litsa-Aragub complex forms a series from diorites to granites and leucogranites.

4. Geochemistry

We have compiled 115 whole-rock geochemical analyses of the Nattanen-type granites. The dataset contains 75 previously unpublished major element analyses from the Nattanen stock (Table 2), 25 major and trace element analyses from all Nattanen-type rocks from The Rock Geochemical Database of Finland (Rasilainen et al., 2007; Appendix 1), and 15 selected granite major element median compositions from Front et al. (1989; Appendix 1). Samples of aplite and rhyolite dykes from the Nattanen intrusion are also included.

Table 2. Major element and zirconium analyses of the Nattanen stock *).

Sample	SiO ₂ (wt.%)	TiO ₂	Al ₂ O ₃	FeOt	MnO	MgO	CaO	Na ₂ O	K ₂ O	P ₂ O ₅	Tot	Zr (ppm)	Ga (ppm)
Nattanen granite (coarse-grained)													
4014-1	74.23	0.15	12.85	1.70	0.01	0.23	0.62	3.50	4.82	0.07	98.18	189	24
4036	72.52	0.33	13.23	2.15	0.03	0.32	0.98	3.64	4.34	0.09	97.63	230	26
4038-1	72.52	0.27	13.23	1.71	0.03	0.27	0.78	3.50	4.70	0.07	97.08	179	27
4040	71.88	0.35	13.04	2.26	0.03	0.35	0.83	3.64	4.70	0.16	97.24	259	27
4042	74.02	0.20	12.85	1.58	0.02	0.17	0.57	3.64	4.70	0.05	97.80	172	29
4048	73.59	0.17	13.23	1.95	0.03	0.32	0.74	3.64	5.06	0.07	98.80	218	25
4050-1	72.1	0.1	13.42	1.32	0.01	0.18	0.76	3.77	4.70	0.14	96.50	117	28
4053	75.09	0.18	12.85	1.68	0.02	0.18	0.62	3.64	4.70	0.07	99.03	190	25
4055-2	73.81	0.18	13.98	2.22	0.02	0.36	0.64	3.50	4.82	0.09	99.62	270	22
4057-1	74.23	0.25	13.79	1.98	0.02	0.28	1.04	3.91	5.06	0.11	100.67	199	26
4060-1	73.16	0.33	13.60	2.38	0.04	0.36	1.11	3.77	4.94	0.11	99.80	269	27
4061-1	75.3	0.25	13.79	1.76	0.02	0.3	0.92	3.91	5.06	0.11	101.42	218	22
4062	74.88	0.28	13.60	1.80	0.04	0.3	0.92	3.91	5.06	0.11	100.9	243	30
4065-1	74.45	0.23	13.42	2.08	0.02	0.3	0.83	3.77	4.94	0.09	100.13	233	30
4066-1	74.02	0.28	13.60	1.79	0.03	0.3	0.91	4.04	4.94	0.14	100.05	208	25
4069-1	75.09	0.33	13.79	2.16	0.03	0.4	0.88	3.77	5.06	0.11	101.62	266	26
4069-2	75.52	0.17	13.23	1.54	0.01	0.15	0.46	3.50	4.82	0.02	99.42	200	25
4074-2	73.16	0.20	13.6	2.75	0.03	0.4	0.73	3.77	4.70	0.14	99.48	277	27
4075-1	75.09	0.25	13.23	1.90	0.02	0.32	0.71	3.64	4.70	0.09	99.95	216	26
4079-1	73.16	0.35	13.98	2.13	0.03	0.33	0.99	3.91	4.58	0.21	99.67	218	25
4082-1	76.16	0.18	13.60	1.57	0.01	0.2	0.60	3.77	4.94	0.18	101.21	185	25
4086	75.09	0.27	12.85	1.63	0.02	0.23	0.76	3.37	4.70	0.18	99.10	192	22
4092	76.16	0.17	13.04	1.50	0.01	0.15	0.76	3.64	4.82	0.23	100.48	150	24
4112	75.3	0.15	12.85	1.25	0.02	0.15	0.5	3.37	4.94	0.11	98.64	150	25
4116	75.09	0.27	13.42	1.67	0.02	0.25	0.85	3.64	4.58	0.09	99.88	161	24
4122-1A	75.73	0.13	13.79	1.17	0.01	0.18	0.74	3.64	4.70	0.25	100.34	109	22
4128	75.09	0.27	13.79	1.86	0.02	0.3	0.74	3.77	4.58	0.09	100.51	215	26
4131-1	74.02	0.27	13.42	1.89	0.02	0.28	0.87	3.77	4.58	0.11	99.23	218	24
4133-1	74.23	0.33	13.04	2.25	0.02	0.33	0.77	3.64	4.58	0.11	99.30	235	23
4222-1	74.23	0.17	13.04	1.59	0.02	0.17	0.46	3.50	4.82	0.00	98.00	180	23
Nattanen granite (medium-grained)													
4003-1A	75.52	0.17	12.66	1.61	0.02	0.40	0.43	3.37	4.94	0.07	99.19	201	23
4003-1B	73.38	0.13	12.66	1.54	0.02	0.15	0.36	3.24	4.82	0.02	96.32	200	22
4005-1	77.44	0.10	12.66	1.07	0.01	0.10	0.41	3.50	4.94	0.18	100.41	86	25
4011-1	73.81	0.12	12.66	1.56	0.01	0.15	0.34	3.37	4.94	0.07	97.03	200	22
4019-1	75.73	0.08	12.85	0.99	0.01	0.05	0.34	3.24	5.18	0.02	98.49	80	20
4028-1	75.09	0.13	12.47	1.61	0.01	0.18	0.66	3.49	4.58	0.27	98.50	164	24
4041-1	73.38	0.12	12.47	1.59	0.01	0.15	0.41	3.50	4.70	0.21	96.54	205	25
4090-1	76.37	0.08	13.04	0.87	0.01	0.07	0.36	3.24	6.26	0.32	100.62	66	28
Nattanen aplite dyke													
4005-2	77.66	0.07	12.85	0.72	0.01	0.03	0.13	4.04	4.46	0.27	100.24	97	30
4122-2	77.02	0.07	12.85	0.66	0.01	0.10	0.43	3.77	4.46	0.32	99.69	79	17
4222-2	75.95	0.10	12.66	0.94	0.03	0.05	0.42	3.77	4.46	0.02	98.40	90	24

Table 2. (cont.)

Sample	SiO ₂ (wt.%)	TiO ₂	Al ₂ O ₃	FeOt	MnO	MgO	CaO	Na ₂ O	K ₂ O	P ₂ O ₅	Tot	Zr (ppm)	Ga (ppm)
Nattanen rhyolite dyke													
4093-1	77.23	0.08	13.04	1.07	0.01	0.05	0.48	3.50	5.18	0.27	100.91	95	27
4107	76.16	0.10	12.66	1.13	0.01	0.03	0.43	3.64	4.46	0.11	98.73	116	26
4111-2	74.66	0.08	12.85	1.04	0.01	0.08	0.35	2.97	5.06	0.21	97.31	132	26
4138-2	75.3	0.10	13.23	1.23	0.03	0.05	0.53	3.77	4.70	0.11	99.05	121	22
4138-3	76.37	0.10	12.66	1.49	0.02	0.08	0.60	3.91	4.46	0.16	99.85	130	26
4140-1	76.59	0.08	13.04	1.05	0.01	0.03	0.41	4.18	4.34	0.25	99.98	93	22
4140-2	75.09	0.05	12.85	1.14	0.03	0.03	0.52	4.31	4.34	0.14	98.50	79	31
4245-1	76.37	0.05	12.85	1.11	0.01	0.02	0.36	3.64	4.58	0.00	98.99	100	25
4247-1	75.09	0.07	13.04	1.18	0.01	0.07	0.28	3.50	4.82	0.00	98.06	100	22
4249-1	75.09	0.07	13.23	0.66	0.01	0.02	0.28	3.91	4.58	0.04	97.89	100	25
4251-1	73.38	0.03	13.23	1.08	0.01	0.02	0.20	3.37	4.70	0.11	96.13	110	31
4262-1	76.16	0.08	13.42	0.85	0.04	0.05	0.41	4.45	3.49	0.23	99.18	100	24
4269-1	74.88	0.05	12.85	0.93	0.01	0.02	0.21	3.64	4.34	0.05	96.98	110	29
4271-1	74.23	0.05	13.04	1.20	0.01	0.07	0.35	3.24	4.94	0.05	97.18	110	20
4289-1	74.23	0.08	12.85	1.32	0.01	0.08	0.32	3.24	4.94	0.05	97.12	120	23
4291-1A	74.45	0.08	12.85	1.08	0.01	0.03	0.22	3.24	4.94	0.14	97.04	110	21
4291-1B	75.30	0.07	12.85	1.12	0.01	0.05	0.22	2.97	5.18	0.02	97.79	120	22
4293-2A	75.73	0.07	13.23	0.80	0.01	0.05	0.15	3.77	4.46	0.02	98.29	110	29
4299-1	75.09	0.07	13.23	0.96	0.02	0.03	0.25	3.91	4.46	0.02	98.04	90	28
4304-1	74.02	0.03	12.85	0.80	0.01	0.03	0.36	3.37	4.94	0.02	96.43	140	25
4306-3	73.81	0.12	13.23	1.22	0.04	0.08	0.8	3.24	5.06	0.07	97.67	160	20
4314-1	75.09	0.08	13.04	0.89	0.01	0.05	0.31	3.37	5.18	0.05	98.07	140	23
4318-1	73.59	0.15	13.04	1.30	0.02	0.03	0.31	3.50	5.66	0.02	97.62	120	21
4318-2	74.23	0.17	13.23	0.62	0.01	0.03	0.38	3.77	4.82	0.02	97.28	140	22
4318-6	75.09	0.10	12.85	1.04	0.01	0.05	0.31	3.24	4.82	0.05	97.56	150	24
4235-1A	76.59	0.05	13.23	0.84	0.06	0.07	0.17	4.04	4.34	0.00	99.39	90	27
4235-1B	76.8	0.08	12.85	1.11	0.03	0.05	0.46	3.37	4.58	0.00	99.33	110	25
4235-2	74.88	0.07	13.04	1.26	0.03	0.10	0.41	3.10	5.42	0.00	98.31	120	24
4231-1	75.09	0.08	12.47	1.16	0.01	0.10	0.35	3.10	4.82	0.00	97.18	140	22
4278-1	75.73	0.10	13.04	0.85	0.01	0.15	0.17	3.37	4.34	0.07	97.83	190	20
4312-2	76.16	0.07	13.23	0.40	0.01	0.03	0.17	3.64	5.06	0.3	99.07	140	23
4335-2A	75.95	0.10	12.85	1.14	0.01	0.15	0.13	2.70	4.46	0.09	97.58	150	22
4363-2	75.3	0.05	12.85	0.93	0.01	0.08	0.11	3.24	4.82	0.07	97.46	110	22
4371-1	75.09	0.03	12.85	0.58	0.01	0.05	0.21	4.04	4.10	0.07	97.03	110	25

*) Methods for data: All major element samples were analysed by atomic absorption spectrophotometer (AAS) at Geological survey of Finland (GTK).

Zr analyses were done by energy dispersive X-ray spectroscopy (EDX), and Ga analyses by optical emission spectrometry (OES) at Geological Survey of Finland (GTK).

4.1. Elemental geochemistry

4.1.1. General description

Figure 4 shows the major element composition of the Nattanen-type granites of Finland. The granites are alkali-calcic to calc-alkaline (Fig. 4a) and marginally peraluminous (A/CNK between 1.0 and about 1.1; Fig. 4b). SiO_2 content is high (~70–78 wt.%) and the Mg# (Fig. 4j) and MgO values are mainly low (0–39 and <0.09–0.76 wt.%, respectively). The Nattanen stock and related aplite and rhyolite dykes are the most evolved, whereas the Vainospää and Riestovaara granites are the least evolved (Fig. 4). TiO_2 , FeOt, MgO and CaO show a negative correlation with SiO_2 (Fig. 4c–f). The Na_2O (2.7–4.7 wt.%) and K_2O (3.5–6.5 wt.%) values are high, CaO values are low (0.1–1.9 wt.%; Fig. 4). K_2O/Na_2O varies between 0.81 and 1.60 (average 1.25).

The Nattanen-type granites show generally high average contents of the LIL elements (Ba 790 ppm, Rb 208 ppm, Sr 153 ppm, Ga (27 ppm), Nb (15 ppm), Th (31 ppm), U (5 ppm) and Zr (219 ppm); compatible trace elements are mostly below the detection limit (Table 3). Figure 5a shows chondrite-normalized REE distributions of the Nattanen-type granites. Overall, the REE contents are rather high for felsic rocks. The REE patterns are steeply fractionated [$(La/Yb)_N \sim 50$ in average] with a moderate negative Eu anomaly ($Eu/Eu^* \sim 0.4$). In primitive mantle-normalized diagrams (Fig. 5b) all the Nattanen-type granites show similar patterns: they are rich in incompatible elements and display negative Ta, Nb, Sr, P and Ti anomalies.

4.1.2. Classification

In previous studies (Haapala et al., 1987; Front et al., 1989), the Nattanen-type granites were considered

as I-type on the basis of mineral composition (magnetite and titanite as characteristic accessory minerals) and the currently available geochemical discrimination criteria (high Na_2O/K_2O , Fig. 6a; relatively weak alumina saturation, Fig. 4b). The authors mentioned that some varieties of these granites show S-type and A-type geochemical characteristics. In the Rb vs. (Y+Nb) classification diagram of Pearce et al. (1984) (Fig. 6b) the Nattanen-type granites plot in the volcanic arc granite field; some of the Vainospää and Riestovaara samples fall, however, into the syn-collisional granite field. According to Pearce (1996) post-collisional granites are difficult to classify with the Rb vs. (Y+Nb) diagram because of their variable source.

In the new classification scheme of Dall'Agnol & Oliveira (2007), designed to separate calc-alkaline granites from A-type granites and oxidized A-type granites from reduced A-type granites, the Nattanen-type granites show a consistent A-type character. In the $CaO/(FeOt+MgO+TiO_2)$ vs. $CaO+Al_2O_3$ (Fig. 6c) and $CaO/(FeOt+MgO+TiO_2)$ vs. Al_2O_3 diagrams (Fig. 6d), the Nattanen-type granites fall mostly in the A-type granite field and they differ clearly from the calc-alkaline granites. However, it should be noted that the Riestovaara and Vainospää granites show partly calc-alkaline (high CaO) characteristics. In the $FeOt/(FeOt+MgO)$ vs. Al_2O_3 (Fig. 6e) and $FeOt/(FeOt+MgO)$ vs. $Al_2O_3/(K_2O/Na_2O)$ diagrams (Fig. 6f), the Nattanen-type granites are transitional between reduced A-type granites, oxidized A-type granites, and calc-alkaline granites, mostly because of their moderate enrichment in FeO relative to MgO. The majority of the Nattanen-type granites are oxidized A-type granites. Rhyolite dykes from the Nattanen stock show strongest the FeOt enrichment compared to MgO and the dykes show reduced A-type characteristics. The Vainospää and Riestovaara

Fig. 4. Composition of the Nattanen, Tepasto, Pomovaara, Riestovaara, and Vainospää granites and related dyke rocks shown in a) Na_2O+K_2O-CaO vs. SiO_2 (fields from Frost et al., 2001); b) A/CNK vs. SiO_2 ; c) TiO_2 vs. SiO_2 ; d) $FeOt$ vs. SiO_2 ; e) MgO vs. SiO_2 ; f) CaO vs. SiO_2 ; g) Na_2O vs. SiO_2 ; h) K_2O vs. Al_2O_3 ; i) P_2O_5 vs. SiO_2 ; j) $Mg\#$ vs. SiO_2 (expressed as cationic proportions, $Mg\# = 100 \times (Mg^{2+} / (Mg^{2+} + Fe^{2+}))$) diagrams.

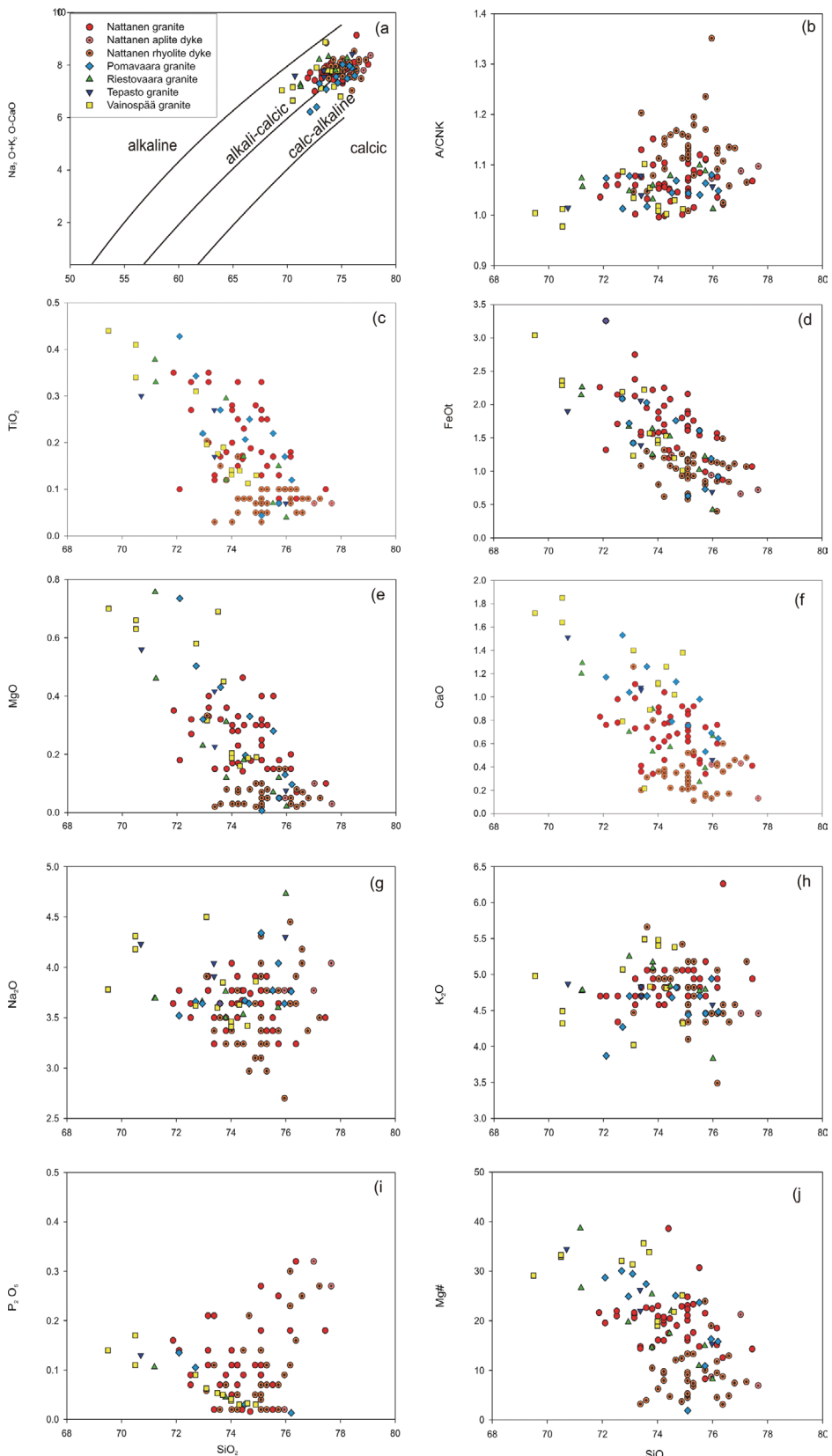


Table 3. TIMS U-Pb isotopic data for zircon, titanite and monazite in Nattanen, Pomovaara, Riestovaara and Vainospää granites

Sample information***		Sample	U	Pb	$^{206}\text{Pb}/^{204}\text{Pb}$	$^{208}\text{Pb}/^{206}\text{Pb}$	ISOTOPIC RATIOS*			Rho**	APPARENT AGES / Ma			
density/size (µm)	(weight/mg)	(ppm)	(ppm)	measured	radiogenic	$^{206}\text{Pb}/^{238}\text{U}$	$2\sigma\%$	$^{207}\text{Pb}/^{235}\text{U}$	$2\sigma\%$	$^{206}\text{Pb}/^{238}\text{U}$	$2\sigma\%$	$^{207}\text{Pb}/^{235}\text{U}$	$2\sigma\%$	$^{207}\text{Pb}/^{206}\text{Pb}$
Sample number (drill core information), location														
A173 (374204/ 7559.9/ 3515.2), Nattanen (Pyhäunturi)														
<i>A173A +70 total</i>	456	581	129	1082	0.25	0.1834	1.0	2.669	1.2	0.10554	0.7	0.812	1085	1319
<i>A173B -70 total</i>	500	603	136	610	0.28	0.1759	1.0	2.528	1.5	0.10423	1.2	0.603	1044	1279
<i>A173C monazite</i>	40	743	2302	4601	10.00	0.3106	1.0	4.625	1.0	0.10799	0.3	0.955	1743	1753
A173D +4.6	21.78	198	59,6	1188	0.30	0.238	1.0	3.516	1.0	0.10714	0.3	0.955	1376	1530
A173E 4.2-4.6	20.82	521	123	964	0.27	0.1896	1.0	2.770	1.1	0.10595	0.4	0.931	1118	1347
A266 (374204/ 7557.95/ 3515.5), Nattanen (Pyhäunturi)														
<i>A266A +160 total</i>	394	875	198	186.6	0.32	0.1461	1.0	2.091	1.7	0.1038	1.5	0.482	879	1145
<i>A266B 70-160</i>	534	840	171	364	0.29	0.1500	1.0	2.123	1.3	0.10264	0.6	0.896	900	1156
<i>A266C -70</i>	300	731	200	287.8	0.55	0.1667	1.0	2.433	1.5	0.10585	1.3	0.520	994	1252
A266D monazite	31	1289	3554	486	9.30	0.3031	1.0	4.553	1.5	0.10894	1.2	0.603	1706	1740
A266E +4.6	20.58	281	67.4	800	0.32	0.1842	1.0	2.727	1.0	0.10737	0.3	0.955	1089	1335
A527 (374204/ 7557.95/ 3516.8), Nattanen (Pyhäunturi)														
A527A (11.0-15.7m) +4.6, +70	19.63	217	66.9	2050	0.28	0.253	1.0	3.730	1.1	0.10692	0.4	0.931	1453	1577
A527B (15.75-32.4m) +4.6, +70	20.92	283	82.7	1208	0.26	0.2393	1.0	3.524	1.0	0.1068	0.3	0.955	1383	1532
A527C (32.-50.0m) +4.6, +70	20.59	278	79.4	1296	0.26	0.2341	1.0	3.446	1.1	0.10676	0.4	0.931	1355	1514
A527D1 (57.70-72m) +4.6, +70	20.78	301	99.8	628	0.26	0.2628	1.0	3.846	1.2	0.10614	0.6	0.866	1504	1602
A527D2 (57.70-72m) +4.6 HF	20.03	154	62.1	3277	0.40	0.3063	1.0	4.610	1.0	0.10915	0.2	0.980	1722	1751
A527E1 (113.5-130.8m) +4.1, 130-160	25.92	672	163	247	0.26	0.174	1.0	2.486	1.2	0.10362	0.7	0.812	1034	1268
A527E2 (113.5-130.8m) +4.6 +70	21.34	243	73.4	1479	0.27	0.247	1.0	3.657	1.0	0.10738	0.3	0.955	1422	1562
A369 (372305/ 7538.0/ 3477.0), Pomovaara														
A369A +4.1 +110	562	600	163	995	0.20	0.2303	1.0	3.434	1.1	0.10814	0.4	0.931	1336	1512
A369B +4.6 +70	19.66	272	90	4271	0.23	0.2846	1.0	4.267	1.0	0.10873	0.3	0.955	1614	1687
A417 (374201/ 7550.6/ 3502.5), Riestovaara (Roviainen)														
A417A +4.6 +160 HF (heterogeneous zircon population)	15.08	234	88.9	890	0.27	0.3015	1.0	4.479	1.0	0.10774	0.3	0.955	1698	1727
A417B 4.2-4.6 +160 HF (heterogenous zircon population)	15.12	328	127	1003	0.26	0.313	1.0	4.642	1.0	0.10756	0.3	0.955	1755	1758

Table 3. (cont.)

A168 (491108/7717.5/4448.0), Vainospää										
<i>A168A 35-70 total</i>	386	1287	258	260	0.29	0.1418	1.0	1.831	1.4	0.09365
<i>A168B +4.2</i>	11.1	1105	215	416	0.24	0.1517	1.0	1.988	1.1	0.09504
<i>A168C titanite</i>	1153	143	59,9	459	0.29	0.3182	1.0	4.756	1.2	0.1084
<i>A168E 4.2-4.6</i>	12.39	1279	263	244	0.29	0.1423	1.0	1.857	1.1	0.09464
										0.4
										0.931
										910
										1111
										1529
										1521
A169 (491108/7717.5/4448.0), Vainospää										
<i>A169A total</i>	293	1061	173	1066	0.20	0.1413	1.0	1.828	1.5	0.09382
<i>A169B +4.2</i>	12.55	942	161	1105	0.20	0.1463	1.0	1.934	1.0	0.09587
<i>A169C titanite</i>	1127	146	61,3	646	0.28	0.3169	1.0	4.744	1.2	0.10857
<i>A169D +4.6</i>	15.93	558	138	1867	0.22	0.2118	1.0	3.042	1.0	0.10416
<i>A169E 4.2-4.6, +70</i>	14.89	1213	246	295	0.26	0.1474	1.0	1.942	1.0	0.09555
<i>A169F 4.2-4.6, +70</i>	15.22	1157	230	354	0.25	0.1497	1.0	1.989	1.4	0.09636
<i>A169G +4.6, 70-160</i>	15.72	796	157	1479	0.21	0.1705	1.0	2.325	1.0	0.0989
<i>A169H +4.6, 70-160</i>	14.66	756	159	1376	0.2	0.1799	1.0	2.475	1.2	0.09977
<i>A169I +4.6, 70-160 HF</i>	13.6	530	138	10539	0.21	0.2273	1.0	3.278	1.0	0.10459
<i>A169J +4.6, -70</i>	15.34	638	149	1570	0.23	0.1967	1.0	2.743	1.0	0.10113
<i>A169K +4.6, abraded</i>	12.13	676	167	1059	0.25	0.20276	1.0	2.833	1.0	0.10133
										0.4
										0.92
										1190
										1364
										1649
A210 (491302/7719.3/4463.9), Vainospää (Pälkänevaara)										
<i>A210A total</i>	337	1226	243	181	0.33	0.1272	1.0	1.678	2.0	0.09567
<i>A210B +4.2</i>	10.15	1064	207	259.5	0.25	0.1402	1.0	1.832	1.1	0.09477
<i>A210D +4.6 +70</i>	16.21	1048	208	273.9	0.25	0.1437	1.0	1.893	1.0	0.09554
<i>A210E 4.2-4.6 +70</i>	14.04	770	159	641	0.2	0.171	1.0	2.358	1.1	0.10001
										0.4
										0.931
										910
										1111
										1529
										1521

A210 (491302/7719.3/4463.9), Vainospää (Pälkänevaara)

A210 (491302/7719.3/4463.9), Vainospää (Pälkänevaara)										
<i>A210A total</i>	337	1226	243	181	0.33	0.1272	1.0	1.678	2.0	0.09567
<i>A210B +4.2</i>	10.15	1064	207	259.5	0.25	0.1402	1.0	1.832	1.1	0.09477
<i>A210D +4.6 +70</i>	16.21	1048	208	273.9	0.25	0.1437	1.0	1.893	1.0	0.09554
<i>A210E 4.2-4.6 +70</i>	14.04	770	159	641	0.2	0.171	1.0	2.358	1.1	0.10001
										0.4
										0.931
										910
										1111
										1529
										1521

Analyses were performed at the Laboratory for Isotope Geology at the Geological Survey of Finland (GTK), Espoo, during 1966-1981. Early analyses carried out by using Borax-fusion are marked in italics (for methods, see Vaasjoki (1977, 2001)).

* Isotopic ratios corrected for fractionation, blank and age related common lead measured from K-feldspar (table 4).

**) Error correlation for $^{207}\text{Pb}/^{235}\text{U}$ vs. $^{206}\text{Pb}/^{238}\text{U}$ ratios.

***) HF: zircons were treated in an ultrasonic cleaner with 5% HF for four minutes (Krogh et al., 1982).

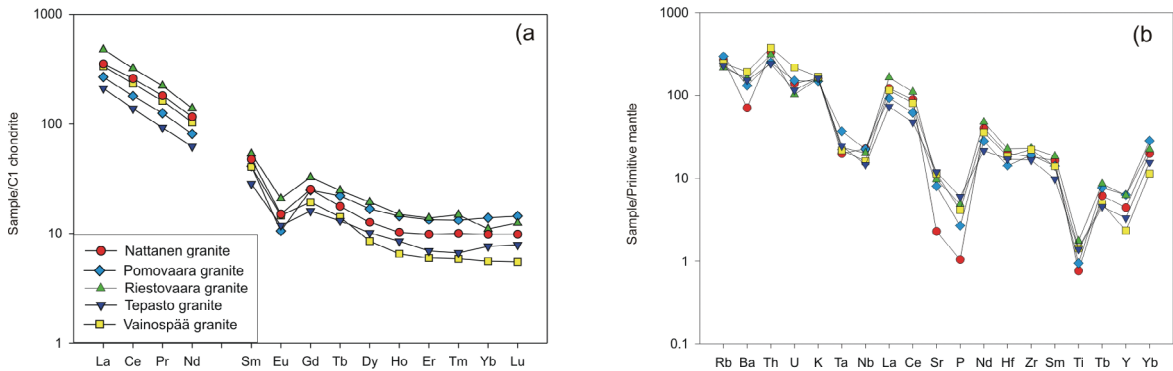


Fig. 5. Trace element composition of representative analyses from Nattanen (92009683), Tepasto (93001676), Pomovaara (92009552), Riestovaara (92009544), and Vainospää (95001306) granites shown in a) chondrite-normalized rare earth elements diagram; b) mantle-normalized spider diagram. Normalization values are from Sun and McDonough (1989).

granites fall between the oxidized A-type and calc-alkaline classes. In the classification scheme of Whalen et al. (1987), the Nattanen-type granites show clear A-type characteristics and fall apart from the S-, M-, and I-type granites, mainly because of their high Ga/Al and Ce values. Obviously, the Nattanen-type granites can be rightfully considered as oxidized A-type granites.

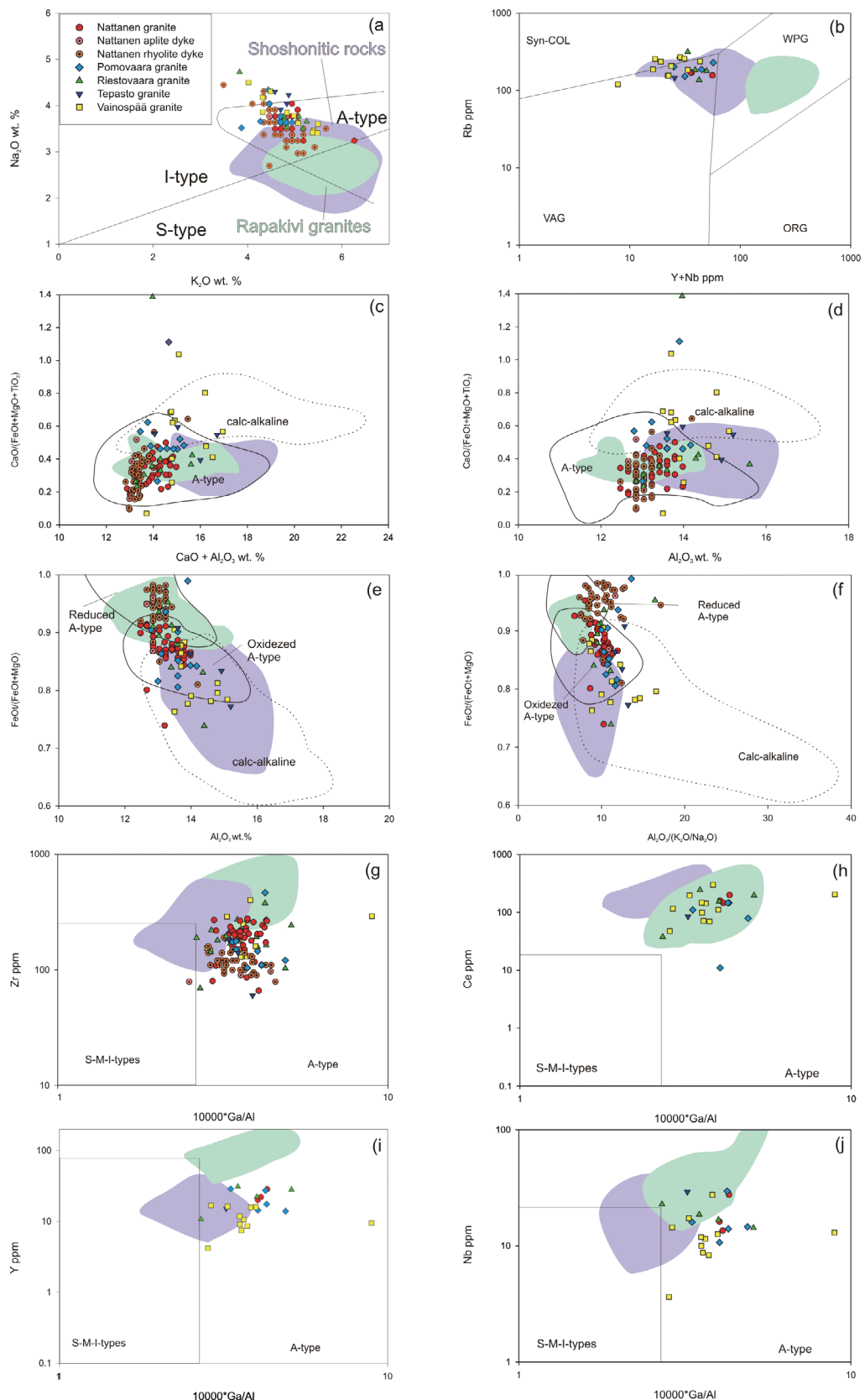
4.2. Zircon saturation thermometry

Zircon saturation temperatures (Watson & Harrison, 1983) calculated for the Nattanen-type granites are in the 720–880 °C range (Fig. 7). Samples from the granite plutons mostly show temperatures above

760 °C, whereas the temperatures calculated for the rhyolitic and aplitic dykes are somewhat lower in average. The U–Pb zircon data acquired for the Nattanen-type granites (e.g., Meriläinen, 1976; Rastas et al., 2001; this volume) indicate that the amount of inherited zircon is very small and thus the calculated zircon saturation temperatures may be considered at least fair estimates of the actual crystallization temperatures (e.g., Miller et al., 2001).

Zircon saturation temperatures after Watson and Harrison (1983) from other geochemically A-type granites in Finland give the following results: the Honkajoki post-kinematic granite in the central Finland granitoid complex 825–900 °C (Elliott, 2001), the Bodom and Obbnäs rapakivi granites in southern

Fig. 6. Classification diagrams of the Nattanen, Tepasto, Pomovaara, Riestovaara, and Vainospää granites and related dykes. a) Na_2O vs. K_2O after White and Chappell (1983). b) Rb vs. $\text{Y}+\text{Nb}$ after (Pearce et al., 1984), abbreviations of the fields: Syn-COL = syncollisional granites; WPG = within-plate granites; VAG = volcanic arc granites; ORG = ocean ridge granites. c) $\text{CaO}/(\text{FeOt}+\text{MgO}+\text{TiO}_2)$ vs. $\text{CaO}+\text{Al}_2\text{O}_3$; d) $\text{CaO}/(\text{FeOt}+\text{MgO}+\text{TiO}_2)$ vs. Al_2O_3 ; e) $\text{FeOt}/(\text{FeOt}+\text{MgO}+\text{TiO}_2)$; f) $\text{FeOt}/(\text{FeOt}+\text{MgO})$ vs. $\text{Al}_2\text{O}_3/(\text{K}_2\text{O}/\text{Na}_2\text{O})$, figures c–f after Dell’Agnol and Oliveira (2007); g) Zr vs. $10000 \times \text{Ga}/\text{Al}$; h) Ce vs. $10000 \times \text{Ga}/\text{Al}$; i) Y vs. $10000 \times \text{Ga}/\text{Al}$; j) Nb vs. $10000 \times \text{Ga}/\text{Al}$, figures g–j after Whalen et al., (1987). Comparison fields after representative ($\text{SiO}_2 > 65$ wt. %) analyses of rapakivi granites from Rämö (1991), Rieder et al. (1996) and Kosunen (1999) (from Wiborg, Bodom, and Obbnäs) and representative ($\text{SiO}_2 > 65$ wt. %) shoshonitic rocks after Rutanen et al. (1997) (from southern Finland and Russian Karelia).



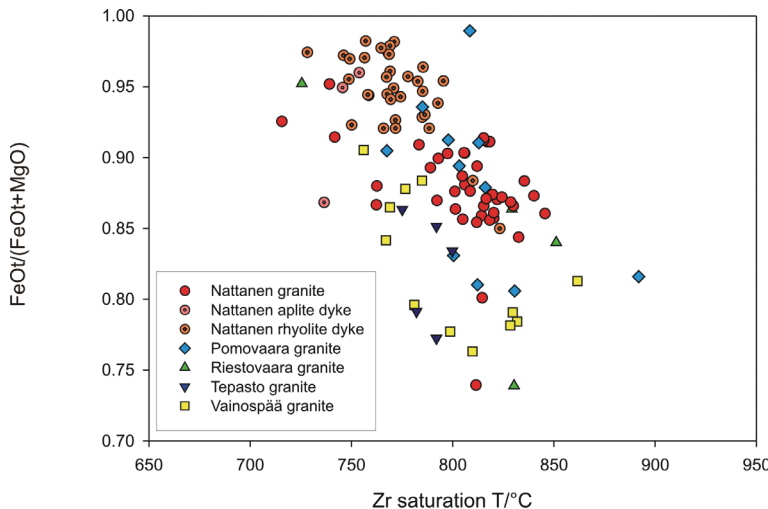


Fig. 7. $\text{FeOt}/(\text{FeOt}+\text{MgO})$ vs. zircon saturation temperature plot for the Nattanen-type granites of Finland. FeOt denotes total iron as FeO , zircon saturation temperatures calculated according to Watson and Harrison (1983).

Finland 830–950 °C (Kosunen, 2004). These are of the same order or slightly higher than the temperatures calculated for the Nattanen-type granites.

5. Isotope geology

In the 1970's isotope geological studies on the Nattanen-type granites were performed at the Isotope Laboratory of the Geological survey of Finland (GTK) in association with a comprehensive dating project (Meriläinen, 1976). Some U–Pb analyses were made already in the 1960's on zircon, monazite, and titanite using the borax-fusion method. These data, comprising 40 U–Pb and 30 Pb–Pb thermal ionization single collector mass spectrometer (TIMS) analyses, are reported in this paper.

5.1. U–Pb results

5.1.1. Nattanen-type intrusions south of the Lapland granulite belt

Twenty one U–Pb analyses on zircon and monazite were made from five granite samples (A173, A266, A527, A369, A417) of the Nattanen, Pomovaara, and Riestovaara plutons located south of the LGB (Ta-

ble 3, sample locations in Fig. 2). The zircon populations in these samples are rather similar and consist predominantly of euhedral, simple, short prisms. The data show that the common Pb content is often high and the results are discordant. All data for the Nattanen-type granites, including two borax-fusion analyses on monazite, plot roughly along a chord that gives intercept ages of 121 ± 43 Ma and 1775 ± 10 Ma (Fig. 8a). In the five samples analyzed, high MSWD of 18 is indicative of substantial scatter in excess of analytical error, which may partly be due to varying zircon populations.

The regression line tilted through the five analyses of Nattanen sample A173 intercept the concordia curve at 109 ± 22 Ma and 1768 ± 6 Ma (MSWD = 1.6; Fig. 8a). The upper intercept relies heavily on a nearly concordant borax-fusion analysis on monazite. The upper intercept age of the Nattanen sample A527 is 1789 ± 5 Ma (MSWD = 2.2), if one analysis with a high common Pb content is excluded. This result is, however, much dependent on analysis A527D2, which has been made from a zircon fraction leached in cold HF, and may thus be biased by unconstrained fractionation. This may also be the case with the two analyses from the Riestovaara (Roivanen) sample A417 (Fig. 8a).

Based on these data we conclude that the age of the Nattanen-type magmatism south of the LGB is ca. 1775 ± 10 Ma in age. The best-fit age result for the Nattanen stock obtained from sample A173 is 1768 ± 6 Ma. The amount of possible xenocrystic zircon within Nattanen-type granitoids is very limited.

5.1.2. Vainospää batholith

The U–Pb data on the Vainospää batholith (Fig. 1, 2) comprises 19 analyses on three samples (Table 3).

The analyzed zircon crystals are pale, euhedral, short, and simple prisms. The analyses show that the common Pb content is typically high and the results are very discordant (Fig. 8b). However, the two analyses on titanite give concordant U–Pb results, yielding an age of 1775 ± 7 Ma. The eleven analyses on sample A169 provide a chord that intercepts the concordia at 346 ± 34 Ma and 1784 ± 20 Ma. The fairly high MSWD of 7.9 suggests some scatter due to geological processes or underestimation of analytical error. Using all nineteen U–Pb analyses from samples

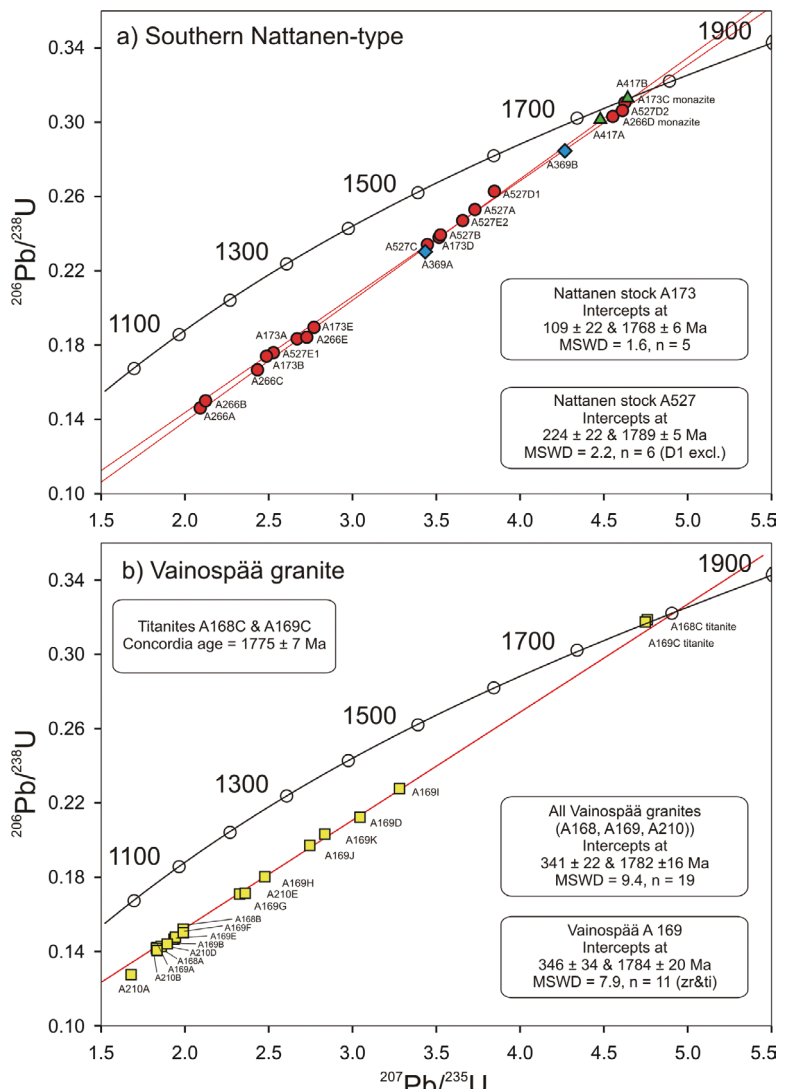


Fig. 8. Concordia diagrams for zircon, monazite, and titanite U–Pb isotope data. a) the Nattanen stock. b) the Vainospää granite.

A168, A169, A210 the intercepts are 341 ± 22 Ma and 1782 ± 16 Ma (MSWD = 9.4; Fig. 8e). From the concordant results obtained for magmatic titanites we conclude that the Vainospää granite crystallized at ca. 1775 ± 7 Ma and that it does not contain appreciable amounts of older xenocrystic zircon.

5.2. Pb–Pb results

Lead isotope analyses on whole-rock and K-feldspar fractions were used to constrain the age and origin of the granites. These data are presented in Table 4 and in the $^{207}\text{Pb}/^{204}\text{Pb}$ vs. $^{206}\text{Pb}/^{204}\text{Pb}$ and $^{208}\text{Pb}/^{204}\text{Pb}$ vs. $^{206}\text{Pb}/^{204}\text{Pb}$ in Fig. 9. The diagrams show the two-stage model of the evolution of crustal lead by Stacey and Kramers (1975) and selected model ratios from the plumbotectonic model of Zartman and Doe (1981).

The data on the Nattanen granites and porphyritic rhyolites (15 analyses on whole rocks, five on K-feldspars) are scattered and do not provide a reliable isochron. Particularly, the most radiogenic analyses of the porphyritic rhyolites (Table 4) suggest late open system behavior and are thus not plotted in figures. For the Nattanen stock, an age of 1719 ± 200 Ma can be calculated from four whole-rocks and four K-feldspar analyses (Fig. 9a). The Pb isotope analyses on three whole rock–K-feldspar pairs from the Vainospää granite yield an age estimate of 1733 ± 87 Ma. The two analyses on whole rock and K-feldspar from the Tepasto granite A184 are consistent with the U–Pb zircon age of ca. 1.8 Ga (Rastas et al., 2001).

Because K-feldspar has a very low U/Pb-ratio and no major metamorphic episodes have affected the Nattanen-type granites since their crystallization, the measured Pb isotopic ratios can be viewed as a reasonable estimate of the initial isotopic composition of the granite. In the case of Nattanen this is relatively unradiogenic ($^{206}\text{Pb}/^{204}\text{Pb} = 14.58$, $^{207}\text{Pb}/^{204}\text{Pb} = 14.85$), particularly in terms of $^{207}\text{Pb}/^{204}\text{Pb}$. The data clearly show that the initial Pb isotope composition (14.80, 15.00) of the Vainospää granite is distinct from the Nattanen granite, but still relatively unradiogenic compared to average crustal lead at 1.7 Ga,

which, according to the model by Stacey and Kramers (1975), has a $^{206}\text{Pb}/^{204}\text{Pb}$ of 15.57 and $^{207}\text{Pb}/^{204}\text{Pb}$ of 15.28 (S&K 1.7 Ga in Fig. 9a). The K-feldspar data plot slightly below (Nattanen) and above (Vainospää) the Zartman and Doe (1981) plumbotectonic model value for the unradiogenic lower crust at 1.8 Ga. The initial isotopic composition of Tepasto granite is more radiogenic than of Nattanen and Vainospää, but less radiogenic than the average terrestrial lead at 1.7 Ga. In the $^{208}\text{Pb}/^{204}\text{Pb}$ vs. $^{206}\text{Pb}/^{204}\text{Pb}$ diagram (Fig. 9b), K-feldspars from Nattanen and Vainospää plot near the Zartman and Doe (1981) lower crust value, which confirms the lower crustal lead isotope signature.

6. Discussion

6.1. Geochemical classification

A-type granites are considered to have crystallized from hot, restite-free and relatively anhydrous magmas (e.g. Loiselle & Wones, 1979; Eby, 1990). Their conspicuous geochemical traits include high alkali abundances, Fe/Mg, Ga/Al, Zr, Nb, Ga, and REE and a negative Eu anomaly. The abundances of CaO, MgO, Sc, Cr, Ni, Ba, Sr, and Eu are generally low (*op. cit.*). A-type granites are most often connected to an extensional tectonic setting, although Whalen et al. (1987) demonstrated that A-type rocks are also found in active subduction zones and transcurrent regimes. Experimental studies suggest that A-type granite magmas may be generated by fluid-absent partial melting of intermediate-felsic rocks involving breakdown of halogen-rich mica and amphibole in mid- to lower crustal pressures and high temperatures (Creaser et al., 1991; Skjerlie & Johnston, 1993). Thus the melting process and source composition may be more important in the genesis of A-type granites than the tectonic setting in which the granites have been emplaced.

The Nattanen-type granites are characterized by high SiO₂, Fe/Mg, LREE, and high contents of incompatible elements (K, Rb, Ba, Th, U). These features point to a crustal source with very little mantle involvement (Figs. 5, 6; Table 2; Appendix 1). This

Table 4. Pb isotope data for Nattanen, Tepasto and Vainospää granites *.

Sample	Location	Wr/ Kfs**	$^{206}\text{Pb}/^{204}\text{Pb}$	$^{207}\text{Pb}/^{204}\text{Pb}$	$^{208}\text{Pb}/^{204}\text{Pb}$	μ_2 ***	Coordinates (WGS85)	
Nattanen granite								
A173	Nattaset	wr	18.61	15.28	41.31		68° 7' 26.712" N	27° 21' 40.569" E
A173Kfs	Nattaset	kfs	14.65	14.85	34.52	1.88	68° 7' 26.712" N	27° 21' 40.569" E
A266Kfs	Nattaset	wr	14.58	14.83	34.48		68° 7' 13.745" N	27° 22' 6.325" E
A349	Salmurinvaara	wr	24.51	15.83	48.59		68° 3' 24.374" N	26° 36' 22.904" E
A350	Lohijoki	wr	18.78	15.33	41.71		67° 57' 35.85" N	26° 58' 10.678" E
A351	Salmurinvaara	wr	21.30	15.44	45.71		68° 2' 42.681" N	26° 38' 20.049" E
A527/10	Nattaset	wr	17.28	15.10	44.32		68° 6' 23.456" N	27° 23' 57.944" E
A527/10Kfs	Nattaset	kfs	14.58	14.84	34.39	1.93	68° 6' 23.456" N	27° 23' 57.944" E
A527/1	Nattaset	wr	17.89	15.19	43.20		68° 6' 23.456" N	27° 23' 57.944" E
A527/12	Nattaset	wr	18.05	15.25	47.14		68° 6' 23.456" N	27° 23' 57.944" E
A527/12Kfs	Nattaset	kfs	14.56	14.87	34.49	1.93	68° 6' 23.456" N	27° 23' 57.944" E
Nattanen porphyric rhyolite dykes								
A307	Vuotso	wr	21.98	15.57	45.44		68° 7' 4.703" N	27° 16' 37.4" E
A307Kfs	Vuotso	kfs	16.20	15.05	36.53	7.85	68° 7' 4.703" N	27° 16' 37.4" E
A345	Hangasjoja	wr	28.87	16.29	63.97			
A346	Tanka-aapa	wr	23.62	15.86	49.11			
A347	Jaurijoki	wr	40.67	17.03	66.19			
A352	Iisinkämppä	wr	198.90	31.48	130.4		68° 7' 23.149" N	26° 19' 21.954" E
A352/2	Iisinkämppä	wr	262.3	37.02	162.87		68° 7' 23.149" N	26° 19' 21.954" E
A353	Vuomaspää	wr	16.72	15.14	38.53			
A354	Ukselmapää	wr	26.50	16.23	27.31			
Tepasto granite								
A184	Kotivaara	wr	20.47	15.73	41.50		67° 59' 55.873" N	24° 40' 27.253" E
A184Kfs	Kotivaara	kfs	15.33	15.17	34.97	1.81	67° 59' 55.873" N	24° 40' 27.253" E
Vainospää granite								
A168	Vainospää	wr	21.00	15.65	43.63		69° 32' 6.656" N	28° 39' 49.136" E
A168Kfs	Vainospää	kfs	14.81	14.99	34.87	1.98	69° 32' 6.656" N	28° 39' 49.136" E
A169	Vainospää	wr	20.05	15.55	41.92		69° 32' 6.656" N	28° 39' 49.136" E
A169Kfs	Vainospää	kfs	14.79	14.98	34.86	1.98	69° 32' 6.656" N	28° 39' 49.136" E
A210	Päkkevaara	wr	16.37	15.16	44.79		69° 33' 39.338" N	29° 4' 11.673" E
A210Kfs	Päkkevaara	kfs	14.82	15.01	34.91	2.01	69° 33' 39.338" N	29° 4' 11.673" E

*) Analyses were made in early 1970s in isotope laboratory of Geological Survey of Finland (GTK), for methods see Vaasjoki (1977).

**) wr = whole rock fraction, kfs = K-feldspar fraction

***) After Stacey and Kramers (1975) two stage model

Isotopic ratios corrected for fractionation using the CIT standard (Catanzaro, 1967), errors 0.2–0.3%.

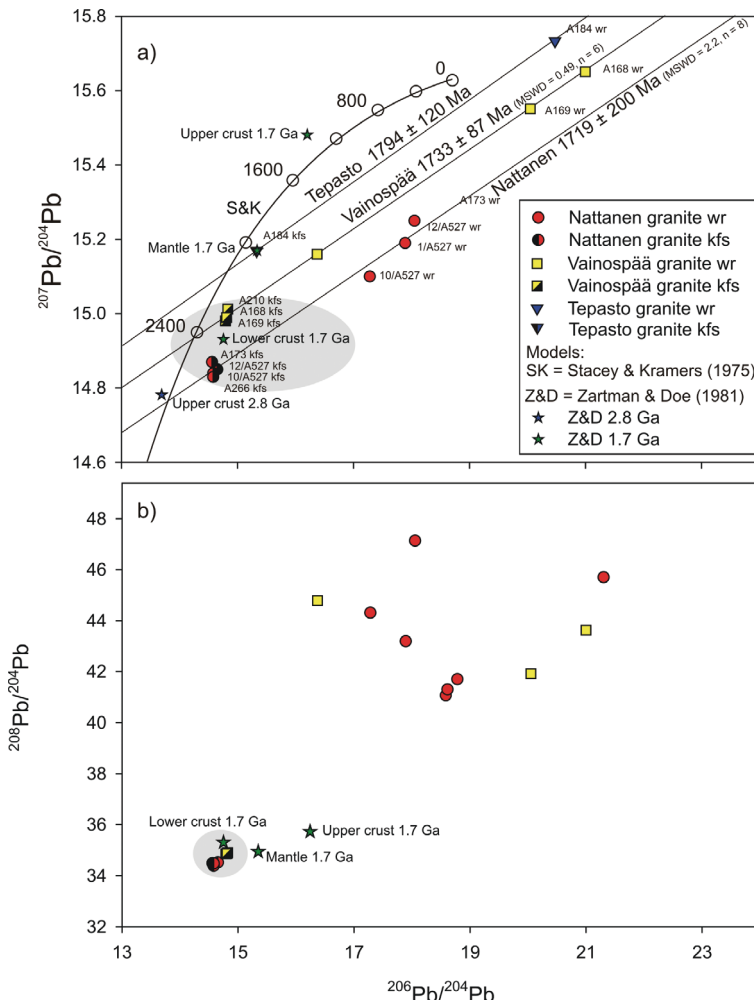


Fig. 9. Kfs = K-feldspar and VR = whole-rock Pb isotope composition of the Nattanen, Tepasto, and Vainospää granites. a) $^{207}\text{Pb}/^{204}\text{Pb}$ vs. $^{206}\text{Pb}/^{204}\text{Pb}$. b) $^{208}\text{Pb}/^{204}\text{Pb}$ vs. $^{206}\text{Pb}/^{204}\text{Pb}$. S&K = evolution curve of the Stacey and Kramers (1975), Z&D = represent mantle, upper crust, and lower crust at 1.7 Ga and 2.8 Ga after Zartman and Doe (1981)

study shows that the Nattanen-type granites have a high Fe/Mg ratio typical for oxidized A-type granites. The rhyolite dykes from the Nattanen stock are more evolved and show reduced A-type characteristics (Fig. 6 c–f; Dall'Agnoll et al., 2007). The up-to-date analyses further allow us to use the classification of Whalen et al. (1987) to confirm the A-type characteristics of the Nattanen-type granites. High Zr saturation temperatures and lack of significant inherited zircon in the Nattanen-type granites also point to an A-type character.

Geochemically, the Nattanen-type granites are similar to the 1.65–1.54 Ga anorogenic, reduced A-type rapakivi granites (e.g., Rämö & Haapala, 2005), and

the ~ 1.8 Ga post-orogenic shoshonitic rocks (e.g., Andersson et al., 2006) of southern Finland. Some differences between these three granite groups can be observed, however. For example, in the tectonic classification of Pearce et al. (1984; Fig. 6b), the Nattanen-type granites and shoshonitic rocks differ from the rapakivi granites in their lower Y+Nb values.

6.2. Petrogenesis

The U–Pb isotopic age data (Table 3, Fig. 8) on zircon, monazite, and titanite indicate that the Nattanen-type granites south of the LGB and the Vainospää granite were emplaced at ca. 1.78 Ga. This is con-

sistent with the 1.80–1.76 Ga ages earlier obtained for the Nattanen-type magmatism in the Fennoscandian shield (Vetrin et al., 2006; Rastas et al., 2001).

The whole-rock and K-feldspar Pb isotope results (Table 4; Fig. 9) suggest that the source of the granites had resided in a relatively low U/Pb environment such as Archean lower crust (Kouvo et al., 1983). The Nattanen and Vainospää K-feldspars plot close to the model Pb isotope ratios for the 1.8 Ga lower crust after Zartman and Doe (1981). The Nattanen-type granitoids are slightly less radiogenic than the Vainospää granite. The K-feldspar data from the Nattanen and the Vainospää plutons are homogeneous implying that Pb was derived from well mixed source before incorporating into the crystallizing rock.

Figure 10 show isotopic variations compared to SiO_2 compositions of the Nattanen, Vainospää, and Tepasto granites. The Nattanen granite shows the strongest crustal isotopic signatures, (least radiogenic initial Hf, Nd and uranogenic Pb isotopic composition) and the most evolved geochemical character. Experimental studies (Watkins et al., 2007) have shown that partial melting of hornblende-bearing (tonalite-trondjemite-granodiorite) TTG in fluid-absent conditions is capable of producing small amounts of peraluminous granitic melts with high SiO_2 and $\text{K}_2\text{O}/\text{Na}_2\text{O}$ at the temperature of <850 °C (0.8–1.2 MPa). An increase in the temperature produces larger vol-

umes of melts of same granitic composition. Zircon saturation temperatures (Fig. 7) for the Nattanen-type granites are in the 720–880°C range, which fits the experimental studies. The high temperatures may have caused melting or resetting of inherited zircons and homogenized Pb–Pb isotope signatures. We suggest that the sources of the Nattanen granites are lower-crustal Archean hornblende-bearing TTG gneisses. High-T melting of low-radiogenic TTG source also explains the homogeneous Pb isotopic characteristics.

Our Pb isotope data are supported by previous Lu–Hf and Sm–Nd isotope studies. Patchett et al. (1981) reported less radiogenic initial ϵ_{Hf} values for the Nattanen granites (-12.1) than for the Vainospää (-9.5) granites (Figs. 10b, 11b), and Huhma (1986) reported lower initial ϵ_{Nd} values for Nattanen (-9.1) than for Vainospää (-8.2; Figs. 10c; 11a). The highest ϵ_{Nd} value was reported for Tepasto (-5.7; Figs. *op. cit.*), which also shows the most radiogenic Pb isotope compositions (Fig. 9a; Fig 10 a), indicating a smaller proportion of Archean source component. The isotopic variation of the different Nattanen-type plutons may be the consequence of varying amounts and nature of source components (U/Pb, Lu/Hf and Sm/Nd ratios and age). For example, Proterozoic metavolcanic rocks in the mainly Archean lower crust could account for the more juvenile character of the Tepas-

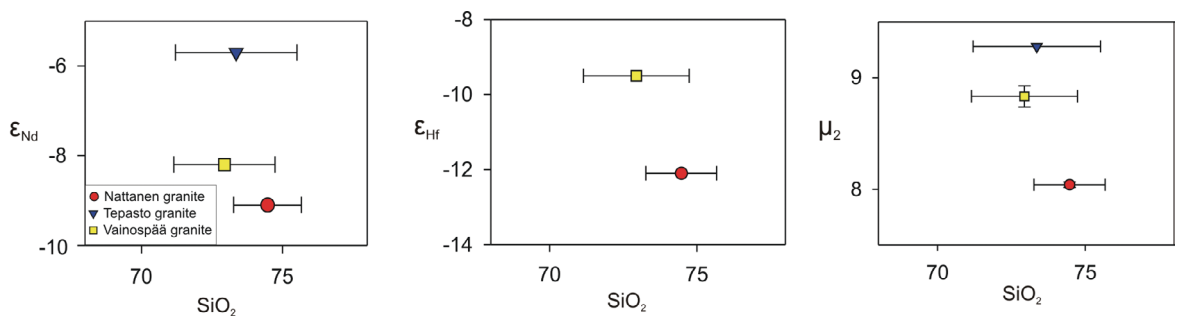


Fig. 10. Isotopic variation compared to average whole-rock composition showing differences of the Nattanen, Tepasto, and Vainospää granites, error bars are standard deviation σ . a) Two stage common lead μ_2 (Stacey & Kramers, 1975) vs. SiO_2 . b) ϵ_{Hf} vs. SiO_2 . c) ϵ_{Nd} vs. SiO_2 .

to granite. This hypothesis is supported by the fact that this batholith is, at the present erosion level, surrounded by Proterozoic rocks (Fig. 1). In addition to different isotopic compositions, some samples of the Vainospää and Tepasto granite show calc-alkaline geochemical features and elevated MgO, CaO and lower SiO₂ than the Nattanen granite, which further implies lithological differences in the source rocks. In summary, the isotopic and geochemical characteristics of the Nattanen-type granites were probably derived from felsic Archean crustal sources (ϵ_{Nd} ca. -13–-10 and ϵ_{Hf} ca. -12.1–-9.5) with minor contributions from younger source components, possibly Proterozoic crust (ϵ_{Nd} ca. -2.5–4.0; Fig. 11a).

A petrogenetic model for the Nattanen-type granites needs to explain their widespread occurrence on both sides of the Kola–Karelia suture. The model should also account for the crustal source, high-T melting conditions, and A-type geochemical character. Experimental studies on the melting of TTG gneisses in high-T conditions (>850 °C at 0.8–1.2 GPa) have produced granitic melts via the breakdown

of amphibole after the exhaustion of biotite and muscovite at lower temperatures (e.g., Watkins et al., 2007 and references therein) that fits well with the isotopic data of the Nattanen-type granites. In here we discuss two plausible tectonic environments that may have produced Nattanen-type granites: extensional setting (e.g. Rämö & Haapala, 2005), and melting of thickened orogenic crust (Vorma, 1976; Windley, 1991). In the case of extensional setting, mafic underplating is the most prominent mechanism and involves heating by mafic mantle derived magmatism and resulting partial melting in the crust, forming the parental magmas of the granites. Partial melting of the mantle may be related to rifting, extensional collapse of orogen, or deep mantle plumes (e.g., Haapala & Rämö, 1999 and references therein). This model is supported by the FIRE 4 seismic reflector profile in Lapland that shows a strong reflection in lower crust (Patison et al., 2006). Similar reflections have been described related to the Finnish rapakivi granites and interpreted as stretching and underplating (Korja & Heikkinen, 1995). This tectonic setting is often regarded as

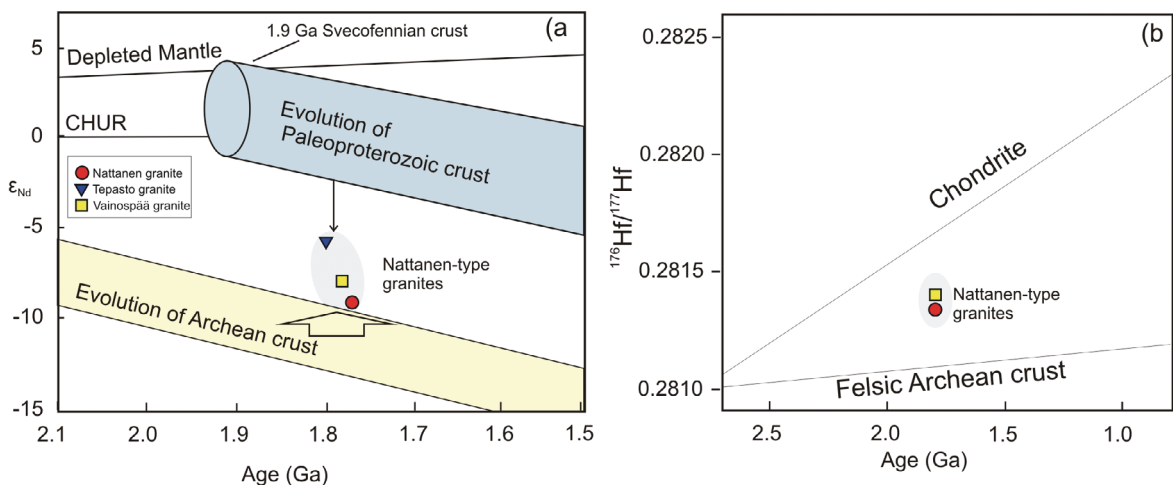


Fig. 11. a) An ϵ_{Nd} vs. age diagram illustrating the Nd isotope evolution of the Nattanen, Tepasto and Vainospää granites. Figure redrawn after Huhma (1986), depleted mantle after DePaolo (1981). b) An $^{176}\text{Hf}/^{177}\text{Hf}$ vs. age diagram illustrating the Hf isotope evolution of the Nattanen and Vainospää granites. Figure redrawn after Patchett et al. (1981). The diagrams show that Nattanen-type granites represent mainly remelted Archean crust, with possible minor contribution from Proterozoic crust.

the regime of A-type granites, but the post-orogenic nature of the Nattanen-type granites (these rocks are partly coeval with orogenic granites of the CLGC; Ahtonen et al., (2007)) calls for also other regimes.

Another plausible tectonic environment, thickened orogenic crust, may have lead to thermal relaxation and is associated with increased radioactive heat production and normalization of the geothermal gradient, leading to high-T partial melting in stacked crust (e.g. Huerta et al., 1996; Vanderhaeghe & Tessier, 2001). A recent study on the thermal evolution of stacked crust in southern Finland suggested that the final products of crustal melting in thickened crust should be geochemically A-type, as higher temperatures are attained in the lower crust, allowing dehydration melting of amphibole to take place (Kukkonen & Lauri, 2009). In the case of the Nattanen-type granites the partial melting of intermediate-felsic crust, involving dehydration break-down of amphibole during thermal relaxation in the lower part of thickened crust is a plausible mechanism for the petrogenesis of the granites, and explains also the lack of observations of coeval, mantle-derived mafic magmatism. The Nattanen-type granites may be geochemically classified as oxidized A-type granites derived from e.g. amphibole-bearing, halogen-enriched rocks of the lower crust, but their tectonic setting can obviously be explained in more than one way.

6.3. Nattanen-type granites and tectonic evolution of the Fennoscandian shield

The tectonic evolution of the Fennoscandian shield was characterized by 2.5–2.0 Ga extension-dominated period in the Early Paleoproterozoic (Vuollo & Huhma, 2005 and references therein). After 2.0 Ga the dominant tectonic events were collisional and the shield grew rapidly by voluminous silicic magmatism that was coeval with the accretion of new terrains to the Archean craton. The collisional period between 1.9–1.8 Ga was a time for extensive crustal growth not only in the Fennoscandian shield but worldwide (e.g., Condie, 2000). The 1.9–1.8 Ga tectonic events have been assigned to the formation of a superconti-

nent (Columbia) that consisted of at least Fennoscandia, Sarmatia, Laurentia, and Amazonia (e.g., Zhao et al., 2002).

The Nattanen-type granites have been considered as post-orogenic (Nironen et al., 2005) relative to the ~1.9–1.8 Ga orogenic activity in Lapland caused by the collision of the Archean Norrbotten, Karelian, and Kola cratons (Lahtinen et al., 2005). Some of the deformed granites of the central Lapland granitoid complex have ages that are similar to or even younger than those of the Nattanen-type granites (Ahtonen et al., 2007), suggesting that the cessation of the collisional tectonics during the emplacement of the Nattanen-type granites was a more local phenomenon than previously thought and that the orogenic activity was not completely over in Lapland by 1.8 Ga.

The situation is similar in southern Finland, where minor shoshonitic post-orogenic granite magmatism (Eklund et al., 1998; Väisänen et al., 2000) was at least partly coeval with the voluminous Svecofennian late-orogenic collision-related leucogranite event between 1.85 Ga and 1.79 Ga (Kurhila et al., 2005; Nironen & Kurhila, 2008). The shoshonitic granites of southern Finland are geochemically similar to the Nattanen-type granites (Fig. 6) and the differences in the geochemistry of the two suites may be a consequence of different sources. The Nattanen-type granites were derived from a dominantly Archean lower crust whereas the shoshonitic rocks of southern Finland have a Paleoproterozoic lithospheric mantle source. Crustal-scale fracture zones in stabilized crust probably explain the locations of the post-orogenic intrusions in the northern and southern parts of the Fennoscandian shield.

7. Conclusions

1. Geochemically the Nattanen-type granites are oxidized, A-type granites and they were derived from a predominantly Archean lower crustal source. They are post-collisional, not anorogenic.
2. U–Pb isotopic age data support the notion that the Nattanen-type granites of Finland and Russia were formed as a consequence of a single magmatic event at 1.80–1.76 Ga.

3. Whole-rock geochemical and isotope geological composition of the Nattanen-type granites suggests derivation mostly from Archean TTG gneisses, involving dehydration breakdown of amphibole. Minor compositional and isotopic differences between the Nattanen-type intrusions reflect varying proportions of different crustal materials in the source.
4. The formation of Nattanen-type granites can be explained at least in two ways:
 - A) Mafic underplating in an extensional setting may have caused high temperature partial melting in the overlying crust, forming the parental magmas of the Nattanen-type granites.
 - B) Postcollisional thermal relaxation, heat production, and stabilization of the geothermal gradient may have led to high temperatures in the thickened crust, and in the resultant formation of the parental magmas of the Nattanen-type granites.
5. In terms of tectonic evolution, the Nattanen-type granites represent the last magmatic event related to the Norbotten, Karelian, and Kola collision.

Acknowledgements

This paper is largely based on a long-term project carried out at the Isotope Laboratory of the Geological Survey of Finland (GTK). We are greatly indebted to Olavi Kouvo who graciously put his isotope data on the Finnish Nattanen-type granites at our disposal and delivered valuable comments on the manuscript. The thorough reviews by Ilmari Haapala and Mikko Nironen are acknowledged. Isotope sample preparation and data reduction were done by the staff of the isotope laboratory. Mirjam Ajlani is thanked for processing Fig. 2. Asko Käpyaho, Paula Kosunen, and Henrikki Rutanen are acknowledged for helping to gather data for the manuscript.

References

- Ahtonen, N., Hölttä, P. & Huhma, H., 2007. Intracratonic Palaeoproterozoic granitoids in northern Finland: prolonged and episodic crustal melting events revealed by Nd isotopes and U–Pb ages on zircon. *Bulletin of Geological Society of Finland* 79, 143–174.
- Andersson, U.B., Eklund, O., Fröjdö, S. & Konopelko, D., 2006. 1.8 Ga magmatism in the Fennoscandian shield; lateral variations in subcontinental mantle enrichment. *Lithos* 86, 110–136.
- Bergman, S., Kubler, L. & Martinsson, O., 2001. Description of regional geological and geophysical maps of northern Norrbotten county (east of the Caledonian orogen), *Sveriges Geologiska Undersökning*. Ser. Ba. Översiktskartor med beskrivningar 56.
- Catanzaro, E.J., 1967. Absolute isotopic abundance ratios of three common lead reference samples. *Earth Planetary Science Letters* 3, 343–346.
- Condie, K.C., 2000. Episodic continental growth models: After thought and extensions. *Tectonophysics* 322, 153–162.
- Creaser, R.A., Price, R.C. & Wormald, R.J., 1991. A-type granites revisited: assessment of a residual-source model. *Geology* 19, 163–166.
- Dall'Agnol, R. & de Oliveira, D.C., 2007. Oxidized, magnetite-series, rapakivi-type granites of Carajás, Brazil: Implications for classification and petrogenesis of A-type granites. *Lithos* 93, 215–233.
- Daly, J.S., Balagansky, V.V., Timmerman, M.J., Whitehouse, M.J., de Jong, K., Guise, P., Bogdanova, S., Gorbatschev, R. & Bridgwater, D., 2001. Ionmicroprobe U–Pb zircon geochronology and isotope evidence for a trans-crustal sutre zone in the Lapland – Kola Orogen, northern Fennoscandian shield. *Precambrian Research* 105, 289–314.
- DePaolo, D.J., 1981. Neodymium isotopes in the Colorado Front Range and crust mantle evolution in Proterozoic. *Nature* 291, 684–696.
- Eby, G.N., 1990. The A-type granitoids; a review of their occurrence and chemical characteristics and speculations on their petrogenesis. *Lithos* 26, 115–134.
- Eklund, O., Konopelko, D., Rutanen, H., Fröjdö, S. & Shebanov, A.D., 1998. 1.8 Ga Svecofennian post-collisional shoshonitic magmatism in the Fennoscandian Shield. *Lithos* 45, 87–108.
- Elliott, B.A., 2001. The petrogenesis of the 1.88–1.87 Ga post-kinematic granitoids of the central Finland granitoid complex. Ph.D. thesis, University of Helsinki, 36 p.
- Elo, S., Lanne, E., Ruotoistenmäki, T. & Sindre, A., 1989. Interpretations of gravity anomalies along the POLAR Profile in the northern Baltic Shield. *Tectonophysics* 162, 135–150.
- Front, K., Vaarma, M., Rantala, E. & Luukkonen, A., 1989. Keski-Lapin varhaisproterotsoiset Nattas-typin graniittikompleksit, niiden kivilajit, geokemia ja mineralisatiot. Summary: Early Proterozoic Nattanen-type granite complexes in central Finnish Lapland: rock types, geochemistry and mineralization. *Geological Survey of Finland, Report of Investigation* 85, 1–77.

- Frost, B.R., Barnes, C.G., Collins, W.J., Arculus, R.J., Ellis, D.J. & Frost, C.D., 2001. A geochemical classification for granitic rocks. *Journal of Petrology* 42, 2033–2048.
- Haapala, I. & Rämö, O.T., 1999. Rapakivi granites and related rocks: an introduction. *Precambrian Research* 95, 1–7.
- Haapala, I., Front, K., Rantala, E. & Vaarma, M., 1987. Petrology of Nattanen-type granite complexes, northern Finland. *Precambrian Research* 35, 225–240.
- Hanski, E. & Huhma, H., 2005. Central Lapland greenstonebelts. Archean rocks. In: Lehtinen, M., Nurmi, P.A. & Rämö, O.T. (eds.) *Precambrian Geology of Finland – Key to the Evolution of the Fennoscandian shield. Developments in Precambrian Geology* 14. Elsevier, Amsterdam, pp. 141–194.
- Huerta A.D., Royden, L.H. & Hodges, K.P., 1996. The Interdependence of Deformational and Thermal Processes in Mountain Belts. *Science* 273, 637–639.
- Huhma, H., 1986. Sm–Nd, U–Pb and Pb–Pb isotopic evidence for the origin of the Early Proterozoic Svecokarelian crust in Finland. *Geological Survey Finland, Bulletin* 337, 1–48.
- Korsman, K., Koistinen, T., Kohonen, J., Wennerström, M., Ekdahl, E., Honkamo, M., Idman, H. & Pekkala, Y., 1997. Bedrock map of Finland 1:1 000 000, Espoo. Geological Survey of Finland.
- Kosunen, P., 1999. The rapakivi granite plutons of Bodom and Obbnäs, southern Finland: petrography and geochemistry. *Bulletin of Geological Society of Finland* 71, 275–304.
- Korja, A. & Heikkinen, P.J., 1995. Proterozoic extensional tectonics of the central Fennoscandian Shield: Results from the Baltic and Bothnian Echoes from the Lithosphere experiments. *Tectonics* 14, 504–517.
- Kosunen, P.J., 2004. Petrogenesis of Mid-Proterozoic A-type granites: case studies from Fennoscandia (Finland) and Laurentia (New Mexico). Ph.D. thesis, University of Helsinki, 21 p.
- Kouvo, O., Huhma, H. & Sakko, M., 1983. Isotopic evidence for old crustal involvement in the genesis of two granites from northern Finland. *Terra Cognita* 3, 135.
- Krogh, T.E., McNutt, R.H. & Davis, G.L., 1982. Two high precision U–Pb zircon ages for the Sudbury Nickel Irruptive. *Canadian Journal of Earth Sciences* 19, 723–728.
- Kukkonen, I.T. & Lauri, L.S., 2009. Modelling the thermal evolution of a collisional Precambrian orogen: High heat production migmatitic granites of southern Finland. *Precambrian Research* 168, 233–246.
- Kurhila, M., Vaasjoki, M., Mänttäri, I., Rämö, O.T. & Nironen, M., 2005. U–Pb ages and Nd isotope characteristics of the lateorogenic, migmatizing microcline granites in southwestern Finland. *Bulletin of the Geological Society of Finland* 77, 105–128.
- Lahtinen, R., Korja, A. & Nironen, M., 2005. Paleoproterozoic tectonic evolution. In: Lehtinen, M., Nurmi, P.A. & Rämö, O.T. (eds.) *Precambrian Geology of Finland – Key to the Evolution of the Fennoscandian shield. Developments in Precambrian Geology* 14. Elsevier, Amsterdam, pp. 481–531.
- Lehtiö, M., 1993. Nattas-typin graniittien raskasmineraalit. Phil. Lic. thesis, University of Helsinki, 117 p.
- Lehtonen, M., Manninen, T., Rastas, P., Väänänen, J., Roos, S.I. & Pelkonen, R., 1985. Keski-Lapin geologisen kartan selitys. Summary: Explanation to the geological map of Central Lapland. Geological Survey of Finland, Report of Investigation 71, 1–35.
- Lehtonen, M., Airo, M.-L., Eilu, P., Hanski, E., Kortelainen, V., Lanne, E., Manninen, T., Rastas, P., Räsänen, J. & Virransalo, P., 1998. Kittilän vihreäkivialueen geologiaa, Lapin vulkaniitti projektin raportti. Summary: The stratigraphy, petrology and geochemistry of the Kittilä greenstone area, northern Finland, A report of the Lapland Volcanite Project. Geological Survey of Finland, Report of Investigation 140, 1–144.
- Loiselle, M.C. & Wones, D.R., 1979. Characteristics and origin of anorogenic granites. *Geological Society of America, Abstracts with Programs* 7, 468.
- Luukkonen, A., 1989. Sodankylän Nattastunturien graniittistokin petrografia, rakenne ja geokemia. Unpublished Mc.S. Thesis, University of Helsinki, 96 p.
- Manninen, T., Pihlaja, P. & Huhma, H., 2001. U–Pb geochronology of the Peurasuvanto area, northern Finland. In: Vaasjoki, M., Radiometric age determinations from Finnish Lapland and their bearing on the timing of Precambrian volcano-sedimentary sequences. Geological Survey of Finland, Special Paper 33, 189–200.
- Meriläinen, K., 1976. The granulite complex and adjacent rocks in Lapland, northern Finland. *Geological Survey of Finland, Bulletin* 281, 1–129.
- Mikkola, E., 1928. Über den Nattanengranit im finnischen Lapplande. *Fennia* 50, 1–22. (in German)
- Mikkola, E., 1941. Suomen geologinen yleiskartta kartta 1:400 000: kallioperäkarttojen selitys lehdet B7-C7-D7 Muonia-Sodankylä-Tuntsajoki. Summary: The General geological map of Finland 1:400 000, explanations to the map of rocks B7-C7-D7 Muonia-Sodankylä-Tuntsajoki. Suomen geologinen toimikunta. 286 p.
- Miller, C.F., Meschter McDowell, S. & Mapes R.W., 2003. Hot and cold granites? Implications of zircon saturation temperatures and preservation of inheritance. *Geology* 31, 529–532.
- Mutanen, T. & Väänänen, J., 2004. PGE-Au-Cu-Ni potential of postkinematic appinitic (1.79 Ga) intrusions in Finland. *Julkaisussa: 17th Australian Geological Convention, Hobart 8–13 February 2004. Dynamic Earth: Past, present, and future. Abstracts.* p. 104.
- Nironen, M., 2005. Proterozoic orogenic granitoid rocks. Paleoproterozoic mafic dikes in NE Finland. In: Lehtinen, M., Nurmi, P.A. & Rämö, O.T. (eds.) *Precambrian Geology of Finland – Key to the Evolution of the Fennoscandian shield. Developments in Precambrian Geology* 14. Elsevier, Amsterdam, pp. 443–479.

- Nironen, M. & Mänttäri, I., 2003. Structural evolution of the Vuotso area, Finnish Lapland. *Bulletin of the Geological Society of Finland* 75, 93–101.
- Nironen, M. & Kurhila, M., 2008. The Veikkola granite area in southern Finland: emplacement of a 1.83–1.82 Ga plutonic sequence in an extensional regime. *Bulletin of the Geological Society of Finland* 80, 39–68.
- Pakkanen, L., 1993. *Kittilän Tepaston graniittikompleksin petrografia, petrofysiikka, geokemia ja Mo-Cu-mineraalisaatio*. Unpublished Mc.S. Thesis, University of Helsinki, 82 p.
- Patison, N.L., Korja, A., Lahtinen, Ojala V.J. & the FIRE Working GROUP, 2006. FIRE seismic reflection profiles 4, 4A and 4B insights into the crustal structure of northern Finland from Ranua to Näätsämö. *Geological Survey of Finland, Special Paper* 43, 161–222.
- Patchett, J., Kouvo, O., Hedge, C. & Tatsumoto, M., 1981. Evolution of continental crust and mantle heterogeneity: evidence from Hf isotopes. *Contributions to Mineralogy and Petrology* 78, 279–297.
- Pearce, J., 1996. Sources and setting of granitic rocks. *Episodes* 19, 120–125.
- Pearce, J.A., Harris, N.B.W. & Tindle, A.G., 1984. Trace element discrimination diagrams for the tectonic interpretations of the granitic rocks. *Journal of Petrology* 25, 956–983.
- Rämö, O.T., 1991. Petrogenesis of the Proterozoic rapakivi granites and related basic rocks of southeastern Fennoscandia: Nd and Pb isotopic and general geochemical constraints. *Geological Survey of Finland, Bulletin* 355, 1–161.
- Rämö, O.T. & Haapala, I., 2005. Rapakivi granites. In: Lehtinen, M., Nurmi, P.A. & Rämö, O.T., (eds.) *Precambrian Geology of Finland – Key to the Evolution of the Fennoscandian shield. Developments in Precambrian Geology* 14. Elsevier, Amsterdam, pp. 553–562.
- Rasilainen, K., Lahtinen, R. & Bornhorst, T.J., 2007. The Rock Geochemical Database of Finland Manual. *Geological Survey of Finland, Report of Investigation* 164, 1–38.
- Rastas, P., Huhma, H., Hanski, E., Lehtonen, M.I., Häkkinen, I., Kortelainen, V., Mänttäri, I. & Paakkola, J.I., 2001. U-Pb isotopic studies on the Kittilä greenstone area, central Lapland, Finland. In: Vaasjoki, M. (ed.) Radiometric age determinations from Finnish Lapland and their bearing on the timing of Precambrian volcano-sedimentary sequences. *Geological Survey of Finland, Special Paper* 33, 95–141.
- Rieder, M., Haapala, I. & Povondra P., 1996. Mineralogy of dark mica from the Wiborg rapakivi batholith, southeastern Finland. *European Journal of Mineralogy* 8, 593–605.
- The Rock Geochemical Database of Finland (online database). Version 1.0. Espoo: Geological Survey of Finland, 30.3.2007. Accessed: 03.06.2007. Available: <http://www.gtk.fi/publ/RGDB>
- Rutanen, H., Eklund, O. & Konopelko, D., 1997. Rock and mineral analyses of Svecofennian postorogenic 1.8 Ga intrusions in southern Finland and Russian Karelia. *Geocenter rapportti – geocenter rapport*, Åbo Akademi University, 8 p.
- Skjerlie, K.P. & Johnston, A.D., 1993. Fluid-absent melting behavior of an F-rich tonalitic gneiss at mid-crustal pressures: implications for the generation of anorogenic granites. *Journal of Petrology* 34, 785–815.
- Stacey, J.S. & Kramers, J.D., 1975. Approximation of terrestrial lead isotope evolution by a two-stage model. *Earth Planetary Science Letters* 26, 207–221.
- Sun, S.S. & McDonough, W.F., 1989. Chemical and isotopic systematic of oceanic basalts: Implications for mantle composition and processes. In: Saunders, A.D. & Norry, M.J. (eds.) *Magmatism, in Ocean basins*. Geological Society of London, Special Publication 42, 313–345.
- Tuisku, P. & Huhma, H., 2006. Evolution of migmatitic granulite complexes: implications from Lapland Granulite Belt, Part II: isotopic dating. *Bulletin of the Geological Society of Finland* 78, 143–175.
- Tuisku, P., Mikkola, P. & Huhma, H., 2006. Evolution of migmatitic granulite complexes: implications from Lapland Granulite Belt, Part 1: metamorphic geology. *Bulletin of the Geological Society of Finland* 78, 71–105.
- Vaasjoki, M., 1977. Rapakivi granites and other postorogenic rocks in Finland: their age and the lead isotopic composition of certain associated galena mineralizations. *Geological Survey of Finland, Bulletin* 294, 1–64.
- Vaasjoki, M., (ed.) 2001. Radiometric age determinations from Finnish Lapland and their bearing on the timing of Precambrian volcano-sedimentary sequences. *Geological Survey of Finland, Special Paper* 33, 1–279.
- Väisänen, M., Mänttäri, I., Kriegsman, L.M. & Höltä, P., 2000. Tectonic setting of post-collisional magmatism in the Palaeoproterozoic Svecofennian orogen, SW Finland. *Lithos* 54, 63–81.
- Vanderhaege, O. & Teyssier, C., 2001. Partial melting and flows of orogens. *Tectonophysics* 342, 451–472.
- Vetrin, V.R., Vinogradov, A.N. & Vinogradov, G.V., 1975. Petrologiya I fatsialno-formatsionnyi analiz litsko-aragubskogo diorite-granitnogo kompleksa. In: Batieve, I.D. (ed.) *Intruzivnye Crarnokity I Porfirovidnye Granity Kolskogo Poluostrova*. Nauka, Apatity, 149–316. (in Russian)
- Vetrin, V.R., Berezhnaya, N.G. & Rodionov, N.V., 2006. Petrology of Postorogenic Granitoids of the Northern Baltic Shield. *Doklady Earth Sciences*, 411A, No 9, 1476–1479.
- Vorma, O., 1976. On the petrochemistry of rapakivi granites with special reference to the Laitila massif, southwestern Finland. *Geological Survey of Finland, Bulletin* 272, 1–98.
- Vuollo, J. & Huhma, H., 2005. Paleoproterozoic mafic dikes in NE Finland. In: Lehtinen, M., Nurmi, P.A. & Rämö, O.T. (eds.) *Precambrian Geology of Finland – Key*

- to the Evolution of the Fennoscandian shield. Developments in Precambrian Geology 14. Elsevier, Amsterdam, pp. 195–236.
- Watkins, J.M., Clemens J.D. & Treloar, P.J., 2007. Archean TTGs as sources of younger granitic magmas: melting of sodic metatonalites at 0.6–1.2 GPa. Contributions to Mineralogy and Petrology 154, 91–110.
- Watson, E.P.B. & Harrison, T.M., 1983. Zircon saturation revisited: temperature and composition effects in a variety of crustal magma types. Earth and Planetary Science Letters 64, 295–304.
- Wennerström, M. & Airo, M.-L., 1998. Magnetic fabric and emplacement of the post-collisional Pomovaara Granite Complex in northern Fennoscandia. Lithos 45, 131–145.
- Whalen, J.B., Currie, K.L. & Chappell, B.W., 1987. A-type granites: geochemical characteristics, discrimination and petrogenesis. Contributions to Mineralogy and Petrology 95, 407–419.
- White, A.J.R. & Chappell, B.W., 1983. Granoid types and their distributions in the Lachlan Fold Belt, south-eastern Australia. In: Roddick, J.A. (ed.) Circum-Pacific Plutons Terraines. Geological Society of America, Memoirs 159, 21–34.
- Windley, B.F., 1991. Early Proterozoic collision tectonics, and rapakivi granites as intrusions in an extensional thrust-thickened crust: the Ketilidian orogen, South Greenland. Tectonophysics 195, 1–10.
- Zartman, R.E. & Doe, B.R., 1981. Plumbotectonics – the model. Tectonophysics 75, 135–162.
- Zhao, G., Cawood, P.A., Wilde, A.S. & Sun, M., 2002. Review of global 2.1–1.8 Ga orogens: implications for a pre-Rodinia supercontinent. Earth-Science Reviews 59, 125–162.

Appendix I. Compiled dataset of previously published whole-rock elemental analyses from granitic samples from Nattanen-type intrusions.

Analyses from The Rock Geochemical Database of Finland (methods are described in Rasilainen et al. (2007))

Appendix I. (cont.)

Intrusion	Nattanen	Nattanen	Nattanen	Pomovaara	Pomovaara	Pomovaara	Pomovaara	Pomovaara	Riestovaara	Riestovaara	Riestovaara	Riestovaara	Riestovaara
Sample	92009679	92009683	92009691	92009552	92009555	92009559	92009561	92009629	92009672	92009569	92009705	92009544	
Na_511p ppm	537	496	564	521	626	636	477	561	433	519	713	488	
Ni_511p ppm	<3	<3	11.4	5.38	<3	6.1	7.25	3.76	3.14	4.84	<3	5.57	
P_511p ppm	81.3	72.9	69.6	225	<50	424	549	70	130	177	<50	469	
Pb_511p ppm	<30	<30	<30	<30	<30	<30	<30	<30	<30	<30	<30	<30	
S_511p ppm	<20	<20	<20	<20	<20	24.9	23.5	<20	<20	<20	<20	155	
Sc_511p ppm	2.62	3.04	2.42	1.79	1.41	2.95	4.45	1.46	2.23	2.23	1.97	2.82	
Sr_511p ppm	1.88	2.4	2.46	7.32	2.29	7.66	5.62	2.56	4.19	4.3	<1	6.46	
Th_511p ppm	41.5	28.8	27.5	29.8	59.2	35.8	64.9	58	37.6	35.9	37.4	31.5	
Ti_511p ppm	160	351	391	638	227	1790	1680	328	730	1470	61.1	1620	
V_511p ppm	<1	3.23	4.14	11.8	<1	23	29.2	2.92	5.13	10.8	<1	28	
Y_511p ppm	20.7	12.5	14.1	21.7	13.8	16.1	23.3	11.9	18.4	23.9	9.32	18.2	
Zn_511p ppm	7.62	5.19	14.6	31.7	8.03	39.6	65.8	11.5	20.4	9.29	8.22	25.5	
Ag_511u ppm	<0.1	<0.1	<0.1	<0.1	<0.1	<0.1	<0.1	<0.1	<0.1	<0.1	<0.1	<0.1	
As_511u ppm	0.333	0.515	0.548	0.785	0.833	0.409	<0.2	0.755	0.47	0.924	0.389	<0.2	
Bi_511u ppm	0.0141	<0.01	0.0114	0.0159	0.0412	0.0159	0.0158	<0.01	0.022	<0.01	<0.01	0.0158	
Sb_511u ppm	<0.03	<0.03	<0.03	<0.03	<0.03	<0.03	<0.03	<0.03	<0.03	<0.03	<0.03	<0.03	
Se_511u ppm	<0.02	<0.02	<0.02	<0.02	<0.02	<0.02	<0.02	<0.02	<0.02	<0.02	<0.02	<0.02	
Au_521u ppb	<0.5	<0.5	<0.5	<0.5	<0.5	<0.5	<0.5	<0.5	<0.5	<0.5	<0.5	<0.5	
Pd_521u ppb	<5	<5	<5	<5	<5	<5	<5	<5	<5	<5	<5	<5	
Te_521u ppb	<10	<10	<10	<10	<10	<10	<10	<10	<10	<10	<10	<10	
F_707i %	0.186	0.109	0.108	0.073	0.024	0.072	0.083	0.045	0.103	0.057	0.09	0.14	
C_811l tot %	<0.01	0.013	<0.01	0.012	0.012	0.016	0.024	0.012	<0.01	0.014	<0.01	0.015	
CO2_816l %	<0.18	<0.18	<0.18	<0.18	<0.18	<0.18	<0.18	<0.18	<0.18	<0.18	<0.18	<0.18	
Cgraf_816l %	<0.05	<0.05	<0.05	<0.05	<0.05	<0.05	<0.05	<0.05	<0.05	<0.05	<0.05	<0.05	
Ce_308m ppm	199	159	146	110	11	146	145	79.1	154	243	37.6	196	
Dy_308m ppm	4.33	3.22	3.61	4.26	1.74	3.08	4.26	1.7	3.28	4.95	0.844	4.92	
Er_308m ppm	2.47	1.63	1.9	2.22	1.13	1.65	2.38	1.28	1.82	2.79	0.771	2.3	
Eu_308m ppm	1.14	0.873	0.825	0.611	0.269	0.8	0.811	0.349	0.88	1.21	<0.1	1.21	
Gd_308m ppm	7.45	5.19	5.14	5.1	1.56	5	5.87	2.22	5.21	8.67	0.946	6.69	
Hf_308m ppm	7.27	6.11	4.88	4.39	5.75	4.47	10.1	3.74	5.35	6.43	4.63	6.99	
Ho_308m ppm	0.834	0.579	0.655	0.818	0.401	0.576	0.881	0.378	0.703	1.08	0.221	0.85	
La_308m ppm	118	83.5	75.5	63.5	5.32	78.2	83.1	48.9	90.9	157	16.9	113	
Lu_308m ppm	0.319	0.25	0.299	0.367	0.223	0.235	0.36	0.26	0.273	0.245	0.268	0.317	
Nb_308m ppm	27.6	16.2	13.5	16	10.7	14	29.6	14.6	16.8	18.6	22.8	14.3	
Nd_308m ppm	72.9	54.3	49.8	37.9	5.5	44.6	50.6	21.2	50.2	82.4	9.19	64.7	
Pr_308m ppm	22.9	17.2	15	11.9	1.46	13.5	16	7.63	16.5	27	3.52	21.2	
Rb_308m ppm	157	171	171	187	203	152	229	266	184	179	317	137	
Sc_308m ppm	4.77	4.8	3.48	3.23	2.06	4.11	6.83	1.59	2.71	1.48	3.89	4.03	
Sm_308m ppm	10.2	7.29	7.05	6.28	1.81	6.26	7.35	2.78	7.12	10.7	1.19	8.19	
Ta_308m ppm	0.83	0.813	0.847	1.51	1.84	0.946	1.76	1.11	1.06	1.04	1.1	0.965	
Tb_308m ppm	0.936	0.663	0.731	0.827	0.239	0.654	0.86	0.326	0.743	1.08	0.15	0.925	
Th_308m ppm	27.2	28.1	23.3	21.2	47.9	23.9	50.9	46.7	25.9	23.9	32.3	26.3	
Tm_308m ppm	0.349	0.255	0.267	0.339	0.213	0.269	0.392	0.191	0.276	0.38	0.174	0.379	
U_308m ppm	3.1	2.94	2.43	3.18	11.8	2.74	4.93	8.6	3.13	2.12	12.6	2.16	
V_308m ppm	1.79	4.01	6.35	11.7	1.13	18.9	26.2	4.32	5.14	7.97	1.61	25.5	
Y_308m ppm	28.4	20.1	22	28.7	14.4	17.5	27.4	13.9	22.3	31	10.7	28.2	
Yb_308m ppm	2.2	1.67	1.94	2.37	1.39	1.83	2.6	1.62	1.84	2.33	1.55	1.87	
Zr_308m ppm	247	185	161	168	158	163	377	103	192	271	69.3	242	

Tepasto	Vainospää												
93001676	95001306	95001302	91011354	91011362	91011365	91011367	91011369	95001281	95001282	95001283	95001307	95001308	
400	400	500	587	647	654	630	824	500	600	500	500	500	
5	5	3.8	3.61	4.2	4.15	4.59	4.83	4	5.8	8.3	6.7	3.9	
594	334	120	168	129	168	214	237	189	425	631	566	104	
<30	<30	<30	<30	<30	<30	<30	<30	<30	<30	<30	<30	<30	
46	<20	<20	<20	<20	<20	<20	<20	<20	<20	318	134	<20	
2.8	1.7	1.6	1.28	1.22	2.19	1.41	1.14	1.8	3.5	1.7	4.3	1.1	
7.1	5.7	6.4	6.24	5.24	5.38	4.96	5.91	7.4	15.1	30.5	15.4	10.5	
26	45	51	52.9	47.6	51.7	55.9	15.6	44	42	46	66	27	
1760	384	565	647	549	780	179	801	728	1410	2250	1730	462	
25.9	17.5	5.1	6.36	5.61	7.11	5.72	10.5	10.5	23.7	27.6	29	14.2	
11.2	8.5	6.8	11.5	6.71	13.6	7.6	3.38	7.4	12.5	7.5	13.1	2.2	
36	19.2	27.6	39.5	30.9	38.4	20.7	39.4	25.7	42.5	17.5	69.1	11.8	
<0.1	0.18	<0.1	<0.1	<0.1	0.211	<0.1	<0.1	<0.1	0.44	<0.1	0.4	<0.1	
0.9	0.6	0.6	0.255	0.359	0.321	<0.2	0.311	0.8	0.9	0.9	0.7	0.5	
0.02	<0.01	<0.01	0.0826	<0.01	<0.01	0.0252	0.033	<0.01	0.02	0.02	<0.01	<0.01	
<0.03	<0.03	<0.03	0.0413	<0.03	0.0421	<0.03	<0.03	<0.03	<0.03	<0.03	<0.03	<0.03	
<0.02	<0.02	<0.02	<0.02	<0.02	<0.02	<0.02	<0.02	<0.02	<0.02	<0.02	<0.02	<0.02	
<0.5	<0.5	<0.5	<0.5	<0.5	<0.5	<0.5	<0.5	<0.5	<0.5	<0.5	<0.5	<0.5	
<5	<5	<5	<5	<5	<5	<5	<5	<5	<5	<5	<5	<5	
<10	<10	<10	<10	<10	<10	<10	<10	<10	<10	<10	<10	<10	
0.04	0.05	0.04	0.04	<0.02	<0.02	<0.02	<0.02	0.05	0.13	0.13	0.14	0.04	
0.02	<0.01	<0.01	<0.01	<0.01	<0.01	<0.01	<0.01	<0.01	<0.01	<0.01	<0.01	<0.01	0.02
<0.18	<0.18	<0.18	<0.18	<0.18	<0.18	<0.18	<0.18	<0.18	<0.18	<0.18	<0.18	<0.18	<0.18
<0.05	<0.05	<0.05	<0.05	<0.05	<0.05	<0.05	<0.05	<0.05	<0.05	<0.05	<0.05	<0.05	<0.05
84.5	143	71.1	111	69.4	116	147	47.4	98.5	196	204	299	71.1	
2.57	2.16	1.39	2.63	1.53	2.74	2.11	0.942	1.74	2.81	1.71	3.26	0.65	
1.15	0.99	0.6	1.37	0.808	1.34	1.05	0.361	0.73	1.3	0.7	1.23	0.2	
0.69	0.85	0.53	0.517	0.376	0.545	0.464	0.402	0.58	0.91	1.2	1.12	0.45	
3.3	3.97	2.99	3.99	2.68	4.43	3.78	1.72	3.56	5.49	4.43	7.64	1.39	
5.29	5.68	3.34	4.53	3.97	4.45	4.89	3.57	4.43	5.99	5.61	10	3.61	
0.48	0.37	0.24	0.473	0.314	0.562	0.413	0.132	0.27	0.5	0.28	0.56	<0.1	
50.1	79.4	42.8	59.6	39.3	65.8	83.2	26.6	57.3	112	123	173	44.3	
0.2	0.14	<0.1	0.201	<0.1	0.2	0.163	<0.1	<0.1	0.15	<0.1	0.13	<0.1	
10.4	11.5	8.75	12.6	8.32	14.4	11.9	3.64	10	17.3	13	27.5	3.1	
29.1	48.3	23.1	35.6	23.9	35.4	45.1	14.6	32.2	61.3	61.6	89.9	20.3	
8.79	15.4	7.15	11.3	7.43	11.5	14.6	4.52	10.2	19.5	20.4	29.7	7.06	
146	155	187	270	256	258	208	120	237	185	156	239	144	
2.98	2.51	1.8	2.99	2.53	2.96	3.17	2.12	3.46	5.28	3.54	4.34	1.46	
4.34	6.20	3.61	5.21	3.50	5.44	5.59	2.24	4.45	7.66	6.7	10.3	2.19	
1.01	0.89	0.49	1.32	0.625	1.19	0.714	0.229	0.48	1.72	0.89	1.35	0.24	
0.49	0.53	0.36	0.521	0.298	0.556	0.526	0.198	0.44	0.69	0.49	0.88	0.18	
20.5	31.9	39.4	41.3	40.4	42.6	51.6	10.4	36	29.8	36	45	19.7	
0.17	0.15	<0.1	0.205	<0.1	0.181	0.174	<0.1	<0.1	0.2	<0.1	0.15	<0.1	
2.43	4.57	12.3	6.83	6.26	5.74	7.64	1.79	6.39	3.15	10.6	1.78	1.91	
23.4	19.5	5.47	7.73	7.06	8.38	10	12.1	12.1	23.1	29.4	26.7	13.1	
15.1	10.6	7.48	16	8.64	16.8	11.8	4.18	9.09	16.2	9.48	15.8	2.9	
1.3	0.95	0.47	1.25	0.661	1.43	1.01	0.311	0.56	1.2	0.62	0.99	0.25	
209	203	113	146	121	152	170	143	161	257	252	383	100	

Median analyses from Front et al. (1989) methods are described in the original publication

Intrusion	Riestovaara coarse porphyritic granite	Riestovaara medium-grained granite	Riestovaara medium-grained granite	Riestovaara granitic porphyry	Riestovaara aplite granite	Riestovaara quartz-feldspar porphyry	Riestovaara Hornblende granodiorite	Pomovaara pothytic granite southern stock	Pomovaara porphyritic granite middle stock	Pomovaara porphyritic granite northern stock	Pomovaara biotite granite	Pomo-vaara aplite granite	Pomo-vaara two-mica granite	Tepasto coarse porphyritic granite	Tepasto biotite granite	Tepasto aplite granite
N	12	22	16	3	6	11	2	20	15	26	6	7	24	10	15	21
SiO ₂ wt.%	71.23	72.94	73.8	75.72	74.44	75.51	68.78	72.95	75.52	73.59	74.66	75.95	75.73	73.37	73.38	75.98
TiO ₂ wt.%	0.33	0.22	0.12	0.15	0.17	0.07	0.37	0.22	0.22	0.27	0.25	0.17	0.07	0.27	0.17	0.07
Al ₂ O ₃ wt.%	14.36	13.6	13.41	12.85	13.03	13.03	14.17	13.98	13.6	14.17	13.6	13.23	14.92	13.98	13.6	
FeOt wt.%	2.26	1.67	1.25	1.22	1.52	1.02	3.93	1.72	1.61	2.03	1.76	1.19	0.73	2.06	1.39	0.69
MnO wt.%	0.02	0.01	0.01	0.00	0.01	0.00	0.06	0.03	0.03	0.03	0.03	0.02	0.01	0.02	0.02	0.01
MgO wt.%	0.46	0.23	0.12	0.12	0.18	0.07	0.74	0.32	0.28	0.43	0.33	0.13	0.05	0.41	0.22	0.07
CaO wt.%	1.29	0.7	0.53	0.39	0.57	0.27	2.18	1.04	0.98	1.26	1.13	0.69	0.53	1.08	1.06	0.46
Na ₂ O wt.%	3.69	3.66	3.76	3.6	3.53	3.77	4.98	3.64	3.77	3.64	3.64	3.64	4.04	4.04	3.91	4.3
K ₂ O wt.%	4.78	5.25	5.09	4.79	4.84	4.77	2.71	4.7	4.7	4.82	4.94	4.46	4.83	4.7	4.58	
Ba (ppm)	1390	1120	758	185	118	1250	1210	900	519	780	1040	328	144	1060	600	60
Sr	188	89	59	b.d.l.	b.d.l.	330	105	100	91	110	133	60	b.d.l.	169	90	b.d.l.
Rb	161	206	216	176	202	94	86	216	248	191	231	245	250	260	273	310
Li	23	17	11	5	5	35	5	27	24	13	28	13	5	56	47	28
Nb	b.d.l.	b.d.l.	b.d.l.	b.d.l.	b.d.l.	b.d.l.	b.d.l.	b.d.l.	b.d.l.	b.d.l.	b.d.l.	b.d.l.	b.d.l.	b.d.l.	b.d.l.	b.d.l.
Zr	189	220	175	196	142	160	295	174	145	150	177	104	110	183	140	60
Ga	20	21	25	22	20	23	25	25	29	25	26	27	29	26	26	28
Sn	b.d.l.	b.d.l.	b.d.l.	b.d.l.	b.d.l.	b.d.l.	b.d.l.	b.d.l.	b.d.l.	b.d.l.	b.d.l.	b.d.l.	b.d.l.	b.d.l.	b.d.l.	b.d.l.
La	77	101	40	28	26	53	28	74	53	78	85	38	7	39	37	6
Y	b.d.l.	b.d.l.	b.d.l.	b.d.l.	b.d.l.	b.d.l.	b.d.l.	b.d.l.	b.d.l.	b.d.l.	b.d.l.	b.d.l.	b.d.l.	b.d.l.	b.d.l.	
Th	25	30	35	24	32	10	14	33	39	49	27	36	34	35	33	16
U	3	3	4	4	4	2	2	4	4	3	5	9	6	7	7	16